

## Simulation studies on $CP$ and $CPT$ violation in $B\bar{B}$ mixing

A. Mohapatra and M. Satpathy  
*Utkal University, Bhubaneswar, Orissa, India*

K. Abe and Y. Sakai  
*KEK, Tsukuba, Ibaraki, Japan 305*  
 (Received 29 January 1998; published 7 July 1998)

A simulation study is carried out for evaluating the experimental sensitivities of the BELLE detector at KEK's  $B$  factory on  $CP$  and  $CPT$  violating effects in  $B^0\bar{B}^0$  mixing.  $CP$  violating effects are examined in terms of the charge asymmetries of same-sign dilepton events and single lepton events. The  $CPT$  violating effect is examined in terms of the time evolution of the opposite-sign dilepton events. As a by-product, it is shown that a precise extraction of the  $B^0\bar{B}^0$  mixing parameter  $x_d$  and the  $B$  lifetime  $\tau_B$  is possible from the proper time distribution of the same-sign dilepton events. [S0556-2821(98)02915-4]

PACS number(s): 11.30.Er, 12.15.Hh, 13.20.He

### I. INTRODUCTION

With the commissioning of  $B$  factories, studies of  $CP$  violation will be extended to a system outside the neutral kaon system for the first time since its 1964 discovery [1]. The potential of  $B$  factories is not limited to an investigation of the origin of  $CP$  violation. A variety of new measurements, especially in the  $CP$ -violating decay modes, can provide alternative ways for exploring new physics. Precision measurements of the time evolution of the  $B^0\bar{B}^0$  system that will become possible in the new facilities provide a new place for testing  $CPT$  invariance in a system where  $CP$  is violated, also for the first time, outside the neutral kaon system.

The  $CP$  violation which was observed in  $K_L \rightarrow \pi\pi$  decays and the charge asymmetry in  $K_L \rightarrow \pi l \nu$  can be consistently explained by introducing a  $CP$ -violating part in the state mixing. While the standard model calculation leads to a magnitude difference between  $K^0 \rightarrow \bar{K}^0$  and  $\bar{K}^0 \rightarrow K^0$  amplitudes that are consistent with the observed effects [2], the equivalent effect in the  $B$  system, namely, a difference between  $B^0 \rightarrow \bar{B}^0$  and  $\bar{B}^0 \rightarrow B^0$  which can show up in the charge asymmetry of same-sign dilepton final states in the  $Y(4S)$  decays, has been generally thought to be too small to observe. Standard model calculations give the size of this asymmetry on the order of  $10^{-3}$  [3–5]. With the start of a new  $B$  factory, however, we expect a significant improvement in this type of measurement. Moreover, it was pointed out by several authors [5–7] that the asymmetry might become as large as  $10^{-2}$ . Among the possible reasons which can cause a larger asymmetry, an interesting possibility is that an effect of new physics is already present in the observed  $B^0\bar{B}^0$  mixing, in addition to the standard model contribution, and the new physics part has a different phase from the standard model part [5,7]. If this is the case, it is possible that we observe a phase of  $M_{12}$  which is quite different from what we expect from the standard model even though the observed magnitude can be consistent with the standard model expectation. It is worthwhile to carefully examine the

sensitivity for the charge asymmetry of same-sign dileptons in future measurements. Besides dileptons, the  $CP$  violation effect can also appear in the charge asymmetry of single leptons [3,8] whose measurement would further enhance the sensitivity for detecting the  $CP$  violation effect [9].

In searching for an effect of  $CPT$  violation, it is natural to look for such effects in a system where  $CP$  is violated [11]. Up to now, such tests have come only from high precision experiments in the neutral kaon system [12]. If  $CP$  is violated in the  $B^0\bar{B}^0$  system, it can provide another way of testing  $CPT$  invariance using quite different experimental techniques [11,13]. A possible difference of the time evolution between  $B^0$  and  $\bar{B}^0$  as a consequence of  $CPT$  violation can be directly detected in the time-dependent charge asymmetry of opposite-sign dilepton events.

The  $B$  factory that is expected to begin operation at KEK (KEKB) [14] in early 1999 is an asymmetric energy  $e^+e^-$  collider. The energy of electron beam and positron beam are set at 8 and 3.5 GeV, respectively. The center-of-mass energy in the collision corresponds to an energy just enough to generate  $Y(4S)$  nearly at rest in the center-of-mass frame. In the detector frame,  $Y(4S)$  moves with a speed of  $\gamma\beta = 0.42$ , and this boost in subsequent decays causes the decay vertices of two  $B$ 's separated typically by 200  $\mu\text{m}$  along the beam direction. From the distance measurements between the two vertices, the proper time of the decay processes can be calculated.  $Y(4S)$  is produced from a photon that has the charge conjugation quantum number  $C = -1$ . The decay of  $Y(4S)$  into  $B\bar{B}$  is a strong interaction process, and therefore  $C$  is conserved. This constraint forces the wave function of  $B^0\bar{B}^0$  pair to evolve in such a way that at any given time one is a charge-conjugate state of the other. This relation makes the measurement of time evolution in the  $B^0\bar{B}^0$  decays possible in spite of the fact that typical separation along the  $z$  direction between two  $B$  decay points ( $\sim 200 \mu\text{m}$ ) is much smaller than the size of interaction region at the beam crossing (0.6 cm). This relation also provides a unique method for flavor tagging. When decay vertices of  $B_1$  and  $B_2$  are

detected at time  $t_1$  and  $t_2$ , respectively, we can determine the flavor of  $B_2$  at  $t_1$  by knowing the flavor of  $B_1$ . The  $B_2$  must have been a charge-conjugate state of  $B_1$  at  $t_1$ . We can know the time evolution of  $B_2$  for the time duration of  $t_2 - t_1$ . The BELLE detector [15] has been designed to provide a good enough position resolution to allow this time evolution. A similar facility at SLAC (BaBar detector and the  $e^+e^-$  storage ring PEP-II) [16] is also expected to begin operation in early 1999. The analysis described in this article can also be performed using this facility.

In Sec. II we present a general formulation for obtaining the joint decay rate of  $B^0\bar{B}^0$  pair produced at  $Y(4S)$  resonance without assuming  $CPT$  invariance. Based on this formulation, we derive expressions for the cases where the final state contains two leptons or single lepton. We then obtain expressions for the charge asymmetries for same-sign dilepton events, single lepton events, and opposite-sign dilepton events. Time dependences for these charge asymmetries are also derived.

Section III describes the method for simulating the  $Y(4S)$  decays and the analysis procedure for obtaining the charge asymmetries and the proper-time distribution. We present sensitivities for  $CP$ - and  $CPT$ -violating effects in the  $B^0\bar{B}^0$  mixing based on the  $100 \text{ fb}^{-1}$  data, although actual simulations were done for  $10^6 Y(4S)$  decays corresponding to  $0.87 \text{ fb}^{-1}$ . The  $100 \text{ fb}^{-1}$  data corresponds to an accumulation during one year running when the accelerator reaches its full design luminosity. In the last section, we compare the expected results from the BELLE experiment with existing results and future prospects from other places.

## II. FORMALISM

### A. Mixing mass matrix and mass eigenstates

The mixing of neutral  $B$  mesons,  $B^0$  and  $\bar{B}^0$  is governed by the  $2 \times 2$  mixing mass matrix:

$$M - \frac{i}{2}\Gamma = \begin{pmatrix} M_{11} - \frac{i}{2}\Gamma_{11} & M_{12} - \frac{i}{2}\Gamma_{12} \\ M_{12}^* - \frac{i}{2}\Gamma_{12}^* & M_{22} - \frac{i}{2}\Gamma_{22} \end{pmatrix}. \quad (1)$$

Here,  $M$  and  $\Gamma$  are Hermitian matrix and these matrix elements are given with Hamiltonian  $H$  as

$$\left( M - \frac{i}{2}\Gamma \right)_{ij} = \langle B_i^0 | H | B_j^0 \rangle \quad (B_1^0 = B^0, B_2^0 = \bar{B}^0). \quad (2)$$

The above mass matrix can be equivalently parametrized in the form [17]

$$M - \frac{i}{2}\Gamma = \begin{pmatrix} -iD + E \cos \theta & E \sin \theta e^{-i\phi} \\ E \sin \theta e^{i\phi} & -iD - E \cos \theta \end{pmatrix}, \quad (3)$$

where  $D$ ,  $E$ ,  $\theta$ , and  $\phi$  are complex parameters and expressed by  $M_{ij}$  and  $\Gamma_{ij}$  as

$$e^{i\phi} = \sqrt{\frac{M_{12}^* - (i/2)\Gamma_{12}^*}{M_{12} - (i/2)\Gamma_{12}}}, \quad (4)$$

$$\cot \theta = \frac{\frac{1}{2}(M_{11} - M_{22}) - (i/4)(\Gamma_{11} - \Gamma_{22})}{\sqrt{[M_{12} - (i/2)\Gamma_{12}][M_{12}^* - (i/2)\Gamma_{12}^*]}}. \quad (5)$$

The  $CPT$  invariance requires diagonal matrix elements to be equal and the  $CP$  invariance further requires the absolute values of off-diagonal matrix elements to be equal, i.e.,

$$\begin{aligned} CPT \text{ invariance: } & M_{11} = M_{22} \quad \text{and} \quad \Gamma_{11} = \Gamma_{22}, \\ & \text{thus} \quad \cot \theta = 0; \end{aligned} \quad (6)$$

$$\begin{aligned} CP \text{ invariance: } & \left| M_{12} - \frac{i}{2}\Gamma_{12} \right| = \left| M_{12}^* - \frac{i}{2}\Gamma_{21}^* \right|, \\ & \text{thus} \quad \text{Im}(\phi) = 0. \end{aligned} \quad (7)$$

Diagonalizing the mass matrix, the mass eigenstates  $|B_H\rangle$  and  $|B_L\rangle$  are given as

$$\begin{aligned} |B_H\rangle &= p|B^0\rangle + q|\bar{B}^0\rangle, \\ |B_L\rangle &= p'|B^0\rangle - q'|\bar{B}^0\rangle, \end{aligned} \quad (8)$$

where the normalizations are

$$|p|^2 + |q|^2 = 1, \quad |p'|^2 + |q'|^2 = 1.$$

$(p, q)$  and  $(p', q')$  are related to the mass matrix elements as

$$\frac{q}{p} = \tan \frac{\theta}{2} e^{i\phi}, \quad \frac{q'}{p'} = \cot \frac{\theta}{2} e^{i\phi}. \quad (9)$$

The masses of above eigenstates are given as

$$\mu_{H/L} = m_{H/L} - \frac{i}{2}\Gamma_{H/L} = -iD \pm E, \quad (10)$$

$$\begin{aligned} \mu &= \frac{1}{2}(\mu_H + \mu_L) = m - \frac{i}{2}\Gamma = -iD \\ &= \frac{1}{2}(M_{11} + M_{22}) - \frac{i}{4}(\Gamma_{11} + \Gamma_{22}), \end{aligned} \quad (11)$$

$$\Delta\mu = \mu_H - \mu_L = \Delta m - \frac{i}{2}\Delta\Gamma = 2E = 2\sqrt{\left( M_{12} - \frac{i}{2}\Gamma_{12} \right) \left( M_{12}^* - \frac{i}{2}\Gamma_{12}^* \right) + \frac{1}{4} \left[ M_{11} - M_{22} - \frac{i}{2}(\Gamma_{11} - \Gamma_{22}) \right]^2}. \quad (12)$$

If  $CPT$  invariance holds, then  $q/p = q'/p'$ . The above formulas reduce to familiar forms:

$$\frac{q}{p} = \frac{q'}{p'} = e^{i\phi} = \sqrt{\frac{M_{12}^* - (i/2)\Gamma_{12}^*}{M_{12} - (i/2)\Gamma_{12}}}, \quad (13)$$

$$\Delta\mu = 2 \sqrt{\left(M_{12} - \frac{i}{2}\Gamma_{12}\right) \left(M_{12}^* - \frac{i}{2}\Gamma_{12}^*\right)}. \quad (14)$$

Note that the following parametrization is usually used in the  $K$ -meson system:

$$p = 1 + \epsilon_1, \quad q = 1 - \epsilon_1, \quad p' = 1 + \epsilon_2, \quad q' = 1 - \epsilon_2, \quad (15)$$

$$\epsilon = (\epsilon_1 + \epsilon_2)/2, \quad \delta = (\epsilon_1 - \epsilon_2)/2. \quad (16)$$

From Eq. (9), when  $|\epsilon| \ll 1$  and  $|\delta| \ll 1$ , Eq. (16) corresponds to

$$\epsilon \cong -\frac{i}{2}\phi, \quad \delta \cong \frac{1}{2}\cos\theta. \quad (17)$$

Since  $\epsilon$  and  $\delta$  depend on the phase conventions and not suitable for sizable  $|\epsilon|$  case which is expected in the  $B$ -meson system, we do not use these parameters in the following.

Using the time evolution of mass eigenstates  $|B_L\rangle$  and  $|B_H\rangle$

$$\begin{aligned} |B_L(t)\rangle &= e^{-(im_L + \Gamma_L/2)t} |B_L(0)\rangle, \\ |B_H(t)\rangle &= e^{-(im_H + \Gamma_H/2)t} |B_H(0)\rangle, \end{aligned} \quad (18)$$

the time evolution of initially pure  $|B^0(t=0)\rangle \equiv |B^0\rangle$  and  $|\bar{B}^0(t=0)\rangle \equiv |\bar{B}^0\rangle$  states are expressed as

$$\begin{aligned} |B^0(t)\rangle &= \left\{ f_+(t) + \frac{c}{d} f_-(t) \right\} |B^0\rangle + 2cq'f_-(t) |\bar{B}^0\rangle \\ &= \{f_+(t) + \cos\theta f_-(t)\} |B^0\rangle + \sin\theta e^{i\phi} f_-(t) |\bar{B}^0\rangle, \end{aligned} \quad (19)$$

$$\begin{aligned} |\bar{B}^0(t)\rangle &= \left\{ f_+(t) - \frac{c}{d} f_-(t) \right\} |\bar{B}^0\rangle + 2cpp'f_-(t) |B^0\rangle \\ &= \{f_+(t) - \cos\theta f_-(t)\} |\bar{B}^0\rangle + \sin\theta e^{-i\phi} f_-(t) |B^0\rangle, \end{aligned} \quad (20)$$

where

$$\begin{aligned} f_+(t) &= e^{-(im + \gamma/2)t} \cos(\Delta\mu t/2), \\ f_-(t) &= ie^{-(im + \gamma/2)t} \sin(\Delta\mu t/2), \end{aligned} \quad (21)$$

$$c = \frac{1}{pq' + qp'}, \quad d = \frac{1}{pq' - qp'}. \quad (22)$$

### B. Joint decay rate of $B^0\bar{B}^0$ pair

The  $B$  mesons are always produced in pairs in  $Y(4S)$  decays. The original  $Y(4S)$  state has quantum number  $J^{PC} = 1^{--}$ . This quantum number is inherited by the  $B\bar{B}$  pair since the decay of  $Y(4S)$  to  $B\bar{B}$  is a strong interaction process, in which both parity and charge conjugation are conserved. This constraint requires that the wave function of the  $B$ -meson pair when created is given by

$$|\Psi(t=0)\rangle = \frac{1}{\sqrt{2}} [ |B^0\rangle |\bar{B}^0\rangle - |\bar{B}^0\rangle |B^0\rangle ]. \quad (23)$$

An expression which governs subsequent time evolution of the pair can be given by substituting Eqs. (19) and (20) into this equation. It can be shown that at any given time the form of Eq. (23) is preserved. This is to say that one is a charge-conjugate state of the other at any given time. Let us consider one of the two neutral  $B$  mesons decay to a final state  $f_a$  at time  $t_1$  and the other to  $f_b$  at time  $t_2$ .  $f_a$  and  $f_b$  may be hadronic or semileptonic states.

The amplitude of this joint decay is written as

$$\begin{aligned} \langle f_a f_b | \Psi(t_1, t_2) \rangle &= \frac{1}{\sqrt{2}} [ \langle f_a | B^0(t_1) \rangle \langle f_b | \bar{B}^0(t_2) \rangle \\ &\quad - \langle f_a | \bar{B}^0(t_1) \rangle \langle f_b | B^0(t_2) \rangle ]. \end{aligned} \quad (24)$$

Substituting the expressions for time evolution for  $B^0(t)$  and  $\bar{B}^0(t)$  from Eqs. (19) and (20) in Eq. (24), and denoting

$$\langle f_i | B^0 \rangle = A_i \quad \text{and} \quad \langle f_i | \bar{B}^0 \rangle = \bar{A}_i$$

the joint amplitude takes the form

$$\begin{aligned}
\langle f_a f_b | \Psi(t_1, t_2) \rangle &= \frac{1}{\sqrt{2}} \left[ \left\{ f_+(t_1) f_+(t_2) - \frac{c^2}{d^2} [f_-(t_1) f_+(t_2)] - 4c^2 p p' q q' f_-(t_1) f_-(t_2) \right\} (A_a \bar{A}_b - \bar{A}_a A_b) \right. \\
&\quad + 2c \{ f_+ [t_1 f_-(t_2) - f_-(t_1) f_+(t_2)] \} (p p' A_a A_b - q q' \bar{A}_a \bar{A}_b) - \frac{c}{d} \{ f_+(t_1) f_-(t_2) - f_-(t_1) f_+(t_2) \} \\
&\quad \left. \times (A_a \bar{A}_b + \bar{A}_a A_b) \right] \\
&= \frac{1}{\sqrt{2}} [ \{ f_+(t_1) f_+(t_2) - \cos^2 \theta [f_-(t_1) f_+(t_2)] - \sin^2 \theta f_-(t_1) f_-(t_2) \} (A_a \bar{A}_b - \bar{A}_a A_b) \\
&\quad + \sin \theta \{ f_+ [t_1 f_-(t_2) - f_-(t_1) f_+(t_2)] \} (e^{-i\phi} A_a A_b - e^{i\phi} \bar{A}_a \bar{A}_b) - \cos \theta \{ f_+(t_1) f_-(t_2) - f_-(t_1) f_+(t_2) \} \\
&\quad \times (A_a \bar{A}_b + \bar{A}_a A_b) ]. \tag{25}
\end{aligned}$$

The joint decay rate is then given as

$$\Gamma[\Psi(t_1, t_2) \rightarrow f_a f_b] = |\langle f_a f_b | \Psi(t_1, t_2) \rangle|^2. \tag{26}$$

Substituting Eq. (25), we obtain

$$\begin{aligned}
\Gamma[\psi(t_1, t_2) \rightarrow f_a f_b] &= \frac{1}{2} e^{-\gamma(t_1+t_2)} \left[ |\cos[\Delta\mu(t_1-t_2)/2]|^2 |A_a \bar{A}_b - \bar{A}_a A_b|^2 + 4|c \sin[\Delta\mu(t_1-t_2)/2]|^2 |p p' A_a A_b - q q' \bar{A}_a \bar{A}_b|^2 \right. \\
&\quad + \left| \frac{c}{d} \sin[\Delta\mu(t_1-t_2)/2] \right|^2 |A_a \bar{A}_b + \bar{A}_a A_b|^2 + 4 \operatorname{Im} \{ c \sin[\Delta\mu(t_1-t_2)/2] \cos[\Delta\mu^*(t_1-t_2)/2] \\
&\quad \times (p p' A_a A_b - q q' \bar{A}_a \bar{A}_b) (A_a \bar{A}_b - \bar{A}_a A_b)^* \} - 2 \operatorname{Im} \left\{ \frac{c}{d} \sin[\Delta\mu(t_1-t_2)/2] \cos[\Delta\mu^*(t_1-t_2)/2] (A_a \bar{A}_b + \bar{A}_a A_b) \right. \\
&\quad \left. \times (A_a \bar{A}_b - \bar{A}_a A_b)^* \right\} - 4 |\sin[\Delta\mu(t_1-t_2)/2]|^2 \operatorname{Re} \left\{ \frac{c c^*}{d^*} (p p' A_a A_b - q q' \bar{A}_a \bar{A}_b) (A_a \bar{A}_b + \bar{A}_a A_b)^* \right\} \left. \right] \\
&= \frac{1}{2} e^{-\Gamma(t_1+t_2)} ( |\cos[\Delta\mu(t_1-t_2)/2]|^2 |A_a \bar{A}_b - \bar{A}_a A_b|^2 + |\sin \theta \sin[\Delta\mu(t_1-t_2)/2]|^2 |e^{-i\phi} A_a A_b - e^{i\phi} \bar{A}_a \bar{A}_b|^2 \\
&\quad + |\cos \theta \sin[\Delta\mu(t_1-t_2)/2]|^2 |A_a \bar{A}_b + \bar{A}_a A_b|^2 + 2 \operatorname{Im} \{ \sin \theta \sin[\Delta\mu(t_1-t_2)/2] \cos[\Delta\mu^*(t_1-t_2)/2] \\
&\quad \times (e^{-i\phi} A_a A_b - e^{i\phi} \bar{A}_a \bar{A}_b) (A_a \bar{A}_b - \bar{A}_a A_b)^* \} - 2 \operatorname{Im} \{ \cos \theta \sin[\Delta\mu(t_1-t_2)/2] \cos[\Delta\mu^*(t_1-t_2)/2] (A_a \bar{A}_b + \bar{A}_a A_b) \\
&\quad \times (A_a \bar{A}_b - \bar{A}_a A_b)^* \} - 2 |\sin[\Delta\mu(t_1-t_2)/2]|^2 \operatorname{Re} \{ \cos \theta^* \sin \theta (e^{-i\phi} A_a A_b - e^{i\phi} \bar{A}_a \bar{A}_b) (A_a \bar{A}_b + \bar{A}_a A_b)^* \} ). \tag{27}
\end{aligned}$$

This is the decay rate of  $B^0 \bar{B}^0$  pair produced at  $Y(4S)$  resonance to the final states  $f_a$  and  $f_b$  without assuming  $CPT$  invariance. The expressions with  $(p, p', q, q')$  and  $(\theta, \phi)$  are simply translated using the relations

$$\frac{c}{d} = \cos \theta, \quad c p p' = \frac{1}{2} \sin \theta e^{-i\phi}, \quad c q q' = \frac{1}{2} \sin \theta e^{i\phi}. \tag{28}$$

Henceforth, we will express all formulas in terms of  $(\theta, \phi)$  only. Decay rates under  $CPT$  invariance can thus be obtained simply by setting  $\cos \theta = 0$  and  $\sin \theta = 1$ :

$$\begin{aligned}
\Gamma[\psi(t_1, t_2) \rightarrow f_a f_b]_{CPT} &= \frac{1}{2} e^{-\Gamma(t_1+t_2)} ( |\cos[\Delta\mu(t_1-t_2)/2]|^2 |A_a \bar{A}_b - \bar{A}_a A_b|^2 \\
&\quad + |\sin[\Delta\mu(t_1-t_2)/2]|^2 |e^{-i\phi} A_a A_b - e^{i\phi} \bar{A}_a \bar{A}_b|^2 \\
&\quad + 2 \operatorname{Im} \{ \sin[\Delta\mu(t_1-t_2)/2] \cos[\Delta\mu^*(t_1-t_2)/2] \\
&\quad \times (e^{-i\phi} A_a A_b - e^{i\phi} \bar{A}_a \bar{A}_b) (A_a \bar{A}_b - \bar{A}_a A_b)^* \} ). \tag{29}
\end{aligned}$$

The physics information contained in the above expressions will become apparent when applied to various cases in the following sections.

### C. Same-sign dilepton charge asymmetry

For obtaining the joint decay rate of  $B^0\bar{B}^0$  pair to positively charged dileptons, we set

$$f_a = (\ell^+ X^-), \quad f_b = (\ell^+ X^-)$$

and assume that the semileptonic decays of  $B$  mesons are flavor specific, i.e.,  $\Delta B = \Delta Q$  and therefore  $B$  mesons ( $\bar{B}$  mesons) always produce positively charged leptons (negatively charged leptons), then

$$\begin{aligned} A_a &= A_b = \langle \ell^+ X^- | B^0 \rangle = A_{\ell} \\ \bar{A}_a &= \bar{A}_b = \langle \ell^+ X^- | \bar{B}^0 \rangle = 0. \end{aligned} \quad (30)$$

Then the decay rate to positively charged dileptons can be derived from Eq. (27) as

$$\begin{aligned} \Gamma_{Y(4S) \rightarrow \ell^+ \ell^+}(t_1, t_2) &= \frac{|A_{\ell}|^4}{2} e^{-\Gamma(t_1+t_2)} |\sin \theta e^{-i\phi} \sin[\Delta\mu(t_1-t_2)/2]|^2 \\ &= \frac{|A_{\ell}|^4}{4} e^{-\Gamma(t_1+t_2)} |\sin \theta e^{-i\phi}|^2 \left[ \cosh\left(\frac{\Delta\Gamma}{2}(t_1-t_2)\right) \right. \\ &\quad \left. - \cos[\Delta m(t_1-t_2)] \right]. \end{aligned} \quad (31)$$

For the second line, we used the relations

$$\begin{aligned} \Delta\mu + \Delta\mu^* &= 2\Delta m, \\ \Delta\mu - \Delta\mu^* &= -i\Delta\Gamma. \end{aligned} \quad (32)$$

If  $CPT$  invariance is assumed, the joint decay rate becomes

$$\begin{aligned} \Gamma_{Y(4S) \rightarrow \ell^+ \ell^+}(t_1, t_2) &= \frac{|A_{\ell}|^4}{4} e^{-\Gamma(t_1+t_2)} |e^{-i\phi}|^2 \left[ \cosh\left(\frac{\Delta\Gamma}{2}(t_1-t_2)\right) \right. \\ &\quad \left. - \cos[\Delta m(t_1-t_2)] \right]. \end{aligned} \quad (33)$$

In the KEKB experiment, we can only measure  $\Delta t = t_1 - t_2$ , not  $t_1$  and  $t_2$  individually. The observable joint decay rate as a function of  $\Delta t$  is obtained by integrating Eq. (31) with  $t_+ = t_1 + t_2$  which is orthogonal to  $\Delta t$ :

$$\begin{aligned} \Gamma_{Y(4S) \rightarrow \ell^+ \ell^+}(\Delta t) &= \frac{|A_{\ell}|^4}{4\Gamma} e^{-\Gamma|\Delta t|} |\sin \theta e^{-i\phi}|^2 \left[ \cosh\left(\frac{\Delta\Gamma}{2}\Delta t\right) \right. \\ &\quad \left. - \cos(\Delta m\Delta t) \right]. \end{aligned} \quad (34)$$

The time-integrated number of the  $\ell^+ \ell^+$  events is given by integrating over  $\Delta t$ ,

$$N^{++} = \frac{|A_{\ell}|^4}{4\Gamma^2} |\sin \theta e^{-i\phi}|^2 \frac{x^2 + y^2}{(1+x^2)(1-y^2)}, \quad (35)$$

where  $x$  and  $y$  are defined as

$$x \equiv \frac{\Delta m}{\Gamma}, \quad y \equiv \frac{\Delta\Gamma}{2\Gamma}. \quad (36)$$

For negatively charged dileptons, we take

$$f_a = (\ell^- X^+), \quad f_b = (\ell^- X^+)$$

so that

$$\begin{aligned} A_a &= A_b = \langle \ell^- X^+ | B^0 \rangle = 0, \\ \bar{A}_a &= \bar{A}_b = \langle \ell^- X^+ | \bar{B}^0 \rangle = \bar{A}_{\ell}. \end{aligned} \quad (37)$$

The joint decay rate in this case is given as

$$\begin{aligned} \Gamma_{Y(4S) \rightarrow \ell^- \ell^-}(t_1, t_2) &= \frac{|\bar{A}_{\ell}|^4}{2} e^{-\Gamma(t_1+t_2)} |\sin \theta e^{i\phi} \sin[\Delta\mu(t_1-t_2)/2]|^2 \\ &= \frac{|\bar{A}_{\ell}|^4}{4} e^{-\Gamma(t_1+t_2)} |\sin \theta e^{i\phi}|^2 \{ \cosh[\Delta\Gamma(t_1-t_2)/2] \\ &\quad - \cos[\Delta m(t_1-t_2)] \}. \end{aligned} \quad (38)$$

The observable joint decay rate as a function of  $\Delta t$  is given as

$$\begin{aligned} \Gamma_{Y(4S) \rightarrow \ell^- \ell^-}(\Delta t) &= \frac{|\bar{A}_{\ell}|^4}{4\Gamma} e^{-\Gamma|\Delta t|} |\sin \theta e^{i\phi}|^2 [ \cosh(\Delta\Gamma\Delta t/2) \\ &\quad - \cos(\Delta m\Delta t) ], \end{aligned} \quad (39)$$

and the time-integrated number of the  $\ell^- \ell^-$  events is given as

$$N^{--} = \frac{|\bar{A}_{\ell}|^4}{4\Gamma^2} |\sin \theta e^{i\phi}|^2 \frac{x^2 + y^2}{(1+x^2)(1-y^2)}. \quad (40)$$

We note here that the  $\ell^+ \ell^+$  and  $\ell^- \ell^-$  events have exactly the same  $\Delta t$  dependence, irrespective of whether  $CPT$  is conserved or not. Thus asymmetry between them does not depend on  $\Delta t$ , and the expression

$$A_{\text{sym}}^{\ell\ell} = \frac{\Gamma_{Y(4S) \rightarrow \ell^+ \ell^+}(\Delta t) - \Gamma_{Y(4S) \rightarrow \ell^- \ell^-}(\Delta t)}{\Gamma_{Y(4S) \rightarrow \ell^+ \ell^+}(\Delta t) + \Gamma_{Y(4S) \rightarrow \ell^- \ell^-}(\Delta t)} \quad (41)$$

becomes equal to

$$A_{\text{sym}}^{\ell\ell} = \frac{|A_{\ell}|^4 |e^{-i\phi}|^2 - |\bar{A}_{\ell}|^4 |e^{i\phi}|^2}{|A_{\ell}|^4 |e^{-i\phi}|^2 + |\bar{A}_{\ell}|^4 |e^{i\phi}|^2} \quad (42)$$

$$= \frac{|e^{-i\phi}|^2 - |e^{i\phi}|^2}{|e^{-i\phi}|^2 + |e^{i\phi}|^2} = \tanh(\text{Im } \phi). \quad (43)$$

In the second line, we assume no direct  $CPT$  violation in the semileptonic decay of  $B^0$  and  $\bar{B}^0$ , i.e.,  $|A_{\ell}|^2 = |\bar{A}_{\ell}|^2$ . Note that  $A_{\text{sym}}^{\ell\ell}$  is exactly the same as the asymmetry of the transition rate of  $B^0\bar{B}^0$  mixing which can be obtained in a straightforward way from Eqs. (19) and (20) and is given as

$$A_{\text{sym}}^{\text{mix}} = \frac{\Gamma(B^0 \rightarrow \bar{B}^0) - \Gamma(\bar{B}^0 \rightarrow B^0)}{\Gamma(B^0 \rightarrow \bar{B}^0) + \Gamma(\bar{B}^0 \rightarrow B^0)} = \frac{|e^{-i\phi}|^2 - |e^{i\phi}|^2}{|e^{-i\phi}|^2 + |e^{i\phi}|^2}. \quad (44)$$

The nonvanishing of  $A_{\text{sym}}^{\text{mix}}$  will imply  $CP$  violation in  $B^0\bar{B}^0$  mixing. In terms of the elements of the mixing mass matrix [Eq. (4)], the asymmetry can be written as

$$A_{\text{sym}}^{\ell\ell} = \frac{\text{Im}(\Gamma_{12}/M_{12})}{1 + \frac{1}{4}|\Gamma_{12}/M_{12}|^2}. \quad (45)$$

#### D. Single leptons charge asymmetry

Let us now consider the case when one of the final states in  $B^0\bar{B}^0$  decay is a lepton and the other may be anything else. Two such cases arise:

$$f_a = (\ell^+ X^-) \quad \text{and} \quad f_b = Y,$$

$$f_a = (\ell^- X^+) \quad \text{and} \quad f_b = Y,$$

where  $Y$  is any state. The general expression for the joint decay rate without assuming  $CPT$  symmetry can be obtained from Eq. (27) and is given as

$$\begin{aligned} \Gamma_{Y(4S) \rightarrow \ell^+ Y} &= \frac{1}{2} e^{-\Gamma(t_1+t_2)} |A_{\ell}|^2 \left( |\cos[\Delta\mu(t_1-t_2)/2]|^2 |\bar{A}_Y|^2 + |\sin[\Delta\mu(t_1-t_2)/2]|^2 |\sin \theta e^{-i\phi} A_Y|^2 \right. \\ &\quad + |\cos \theta \sin[\Delta\mu(t_1-t_2)/2]|^2 |\bar{A}_Y|^2 + 2 \text{Im}\{\sin[\Delta\mu(t_1-t_2)/2] \cos[\Delta\mu^*(t_1-t_2)/2] \sin \theta e^{-i\phi} A_Y \bar{A}_Y^*\} \\ &\quad - 2 \text{Im}\{\cos \theta \sin[\Delta\mu(t_1-t_2)/2] \cos[\Delta\mu^*(t_1-t_2)/2] \bar{A}_Y \bar{A}_Y^*\} - 2 |\sin[\Delta\mu(t_1-t_2)/2]|^2 \\ &\quad \left. \times \text{Re}\{\cos \theta^* \sin \theta e^{-i\phi} A_Y \bar{A}_Y^*\} \right). \end{aligned} \quad (46)$$

In terms of  $\Delta\Gamma$  and  $\Delta m$  the above expression takes the form

$$\begin{aligned} \Gamma_{Y(4S) \rightarrow \ell^+ Y} &= \frac{|A_{\ell}|^2}{4} e^{-\gamma(t_1+t_2)} \left[ \cos[\Delta m(t_1-t_2)] \sum_Y \{ (1 - |\cos \theta|^2) |\bar{A}_Y|^2 - |\sin \theta e^{-i\phi}|^2 |A_Y|^2 + \sin \theta e^{-i\phi} A_Y \bar{A}_Y^* \cos \theta^* \right. \\ &\quad + \sin \theta^* e^{i\phi} A_Y^* \bar{A}_Y \cos \theta \} + \cosh[\Delta\Gamma(t_1-t_2)/2] \sum_Y \{ (1 + |\cos \theta|^2) |\bar{A}_Y|^2 + |\sin \theta e^{-i\phi}|^2 |A_Y|^2 \\ &\quad - \sin \theta e^{-i\phi} A_Y \bar{A}_Y^* \cos \theta^* - \sin \theta^* e^{i\phi} A_Y^* \bar{A}_Y \cos \theta \} + \sin[\Delta m(t_1-t_2)] \sum_Y \{ -i \sin \theta e^{-i\phi} A_Y \bar{A}_Y^* \\ &\quad + i \sin \theta^* e^{-i\phi} A_Y^* \bar{A}_Y + i(\cos \theta - \cos \theta^*) |\bar{A}_Y|^2 \} - \sinh[\Delta\Gamma(t_1-t_2)/2] \sum_Y \{ \sin \theta e^{-i\phi} A_Y \bar{A}_Y^* \\ &\quad \left. + \sin \theta^* e^{i\phi} A_Y^* \bar{A}_Y - (\cos \theta - \cos \theta^*) |\bar{A}_Y|^2 \} \right]. \end{aligned} \quad (47)$$

Now we want to integrate over  $t_1$  and sum over all final states  $Y$ :

$$\Gamma_{Y(4S) \rightarrow \ell^+}(t_2) = 2 \sum_Y \int_0^\infty \Gamma_{Y(4S) \rightarrow \ell^+ Y}(t_1, t_2) dt_1. \quad (48)$$

The factor 2 accounts for the fact that the final state  $Y$  can come from either side of the  $Y(4S)$  decay:

$$\begin{aligned}
\Gamma_{Y(4S) \rightarrow \ell^+}(t_2) &= \frac{|A_{\ell}|^2}{4\Gamma} e^{-\Gamma t_2} \left[ \left\{ \frac{1}{1+x^2} \cos(\Delta m t_2) + \frac{x}{1+x^2} \sin(\Delta m t_2) \right\} \times \sum_Y \{ (1 - |\cos \theta|^2) |\bar{A}_Y|^2 - |\sin \theta e^{-i\phi}|^2 |A_Y|^2 \right. \\
&\quad \left. + \sin \theta e^{-i\phi} A_Y \bar{A}_Y^* \cos \theta^* + \sin \theta^* e^{-i\phi^*} A_Y^* \bar{A}_Y \cos \theta \right\} + \left\{ \frac{1}{1-y^2} \cosh(\Delta \Gamma t_2/2) - \frac{y}{1-y^2} \sinh(\Delta \Gamma t_2/2) \right\} \\
&\quad \times \sum_Y \{ (1 + |\cos \theta|^2) |\bar{A}_Y|^2 + |\sin \theta e^{-i\phi}|^2 |A_Y|^2 - \sin \theta e^{-i\phi} A_Y \bar{A}_Y^* \cos \theta^* - \sin \theta^* e^{-i\phi^*} A_Y^* \bar{A}_Y \cos \theta \} \\
&\quad + \left\{ \frac{x}{1+x^2} \cos(\Delta m t_2) - \frac{1}{1+x^2} \sin(\Delta m t_2) \right\} \sum_Y \{ -i \sin \theta e^{-i\phi} A_Y \bar{A}_Y^* + i \sin \theta^* e^{-i\phi^*} A_Y^* \bar{A}_Y \\
&\quad + i(\cos \theta - \cos \theta^*) |\bar{A}_Y|^2 \} - \left\{ \frac{y}{1-y^2} \cosh(\Delta \Gamma t_2/2) - \frac{1}{1-y^2} \sinh(\Delta \Gamma t_2/2) \right\} \\
&\quad \times \sum_Y \{ \sin \theta e^{-i\phi} A_Y \bar{A}_Y^* + \sin \theta^* e^{-i\phi^*} A_Y^* \bar{A}_Y - (\cos \theta + \cos \theta^*) |\bar{A}_Y|^2 \} \Big]. \tag{49}
\end{aligned}$$

Using the relation

$$\sum_Y |\langle Y | \psi \rangle|^2 = - \frac{d}{dt} \langle \psi | \psi \rangle \tag{50}$$

and putting  $B^0$  and  $\bar{B}^0$  for  $\psi$ , we get a series of relations which are derived in the Appendix. Using the relations given by Eqs. (A8)–(A11) in Eq. (49), the dependence of joint decay rate on the final state  $Y$  is eliminated and one obtains

$$\begin{aligned}
\Gamma_{Y(4S) \rightarrow \ell^+}(t_2) &= \frac{|A_{\ell}|^2}{4} e^{-\Gamma t_2} \left[ \cos(\Delta m t_2) \left\{ \frac{1-x^2}{1+x^2} (1 - |\cos \theta|^2 - |\sin \theta e^{-i\phi}|^2) + \frac{2ix}{1+x^2} (\cos \theta - \cos \theta^*) \right\} \right. \\
&\quad \left. + \cosh\left(\frac{\Delta \Gamma t_2}{2}\right) \left\{ \frac{1+y^2}{1-y^2} (1 + |\cos \theta|^2 + |\sin \theta e^{-i\phi}|^2) + \frac{2y}{1-y^2} (\cos \theta + \cos \theta^*) \right\} \right. \\
&\quad \left. + \sin(\Delta m t_2) \left\{ \frac{2x}{1+x^2} (1 - |\cos \theta|^2 - |\sin \theta e^{-i\phi}|^2) - i \frac{1-x^2}{1+x^2} (\cos \theta - \cos \theta^*) \right\} \right. \\
&\quad \left. - \sinh\left(\frac{\Delta \Gamma t_2}{2}\right) \left\{ \frac{2y}{1-y^2} (1 + |\cos \theta|^2 + |\sin \theta e^{-i\phi}|^2) + \frac{1+y^2}{1-y^2} (\cos \theta + \cos \theta^*) \right\} \right]. \tag{51}
\end{aligned}$$

A similar expression can be obtained for negatively charged single lepton case. This is given as

$$\begin{aligned}
\Gamma_{Y(4S) \rightarrow \ell^-}(t_2) &= \frac{|A_{\ell}|^2}{4} e^{-\Gamma t_2} \left[ \cos(\Delta m t_2) \left\{ \frac{1-x^2}{1+x^2} (1 - |\cos \theta|^2 - |\sin \theta e^{i\phi}|^2) - \frac{2ix}{1+x^2} (\cos \theta - \cos \theta^*) \right\} \right. \\
&\quad \left. + \cosh\left(\frac{\Delta \Gamma t_2}{2}\right) \left\{ \frac{1+y^2}{1-y^2} (1 + |\cos \theta|^2 + |\sin \theta e^{i\phi}|^2) - \frac{2y}{1-y^2} (\cos \theta + \cos \theta^*) \right\} \right. \\
&\quad \left. + \sin(\Delta m t_2) \left\{ \frac{2x}{1+x^2} (1 - |\cos \theta|^2 - |\sin \theta e^{i\phi}|^2) + i \frac{1-x^2}{1+x^2} (\cos \theta - \cos \theta^*) \right\} \right. \\
&\quad \left. - \sinh\left(\frac{\Delta \Gamma t_2}{2}\right) \left\{ \frac{2y}{1-y^2} (1 + |\cos \theta|^2 + |\sin \theta e^{i\phi}|^2) - \frac{1+y^2}{1-y^2} (\cos \theta + \cos \theta^*) \right\} \right]. \tag{52}
\end{aligned}$$

Here we have made use of the relations given in Eqs. (A12)–(A15) to eliminate  $Y$ . Let us denote the total expected number of  $\ell^+$  and  $\ell^-$  states in the decay process as  $N^+$  and  $N^-$ , respectively. These are defined as

$$N^+ = \int_0^\infty \Gamma_{Y(4S) \rightarrow \ell^+(t_2)} dt_2, \quad (53)$$

$$N^- = \int_0^\infty \Gamma_{Y(4S) \rightarrow \ell^-(t_2)} dt_2. \quad (54)$$

Substituting Eqs. (52) and (53) in Eqs. (53) and (54), respectively, and carrying out the integrations over  $t_2$ ,  $N^+$  and  $N^-$  are obtained as

$$N^+ = \frac{|A_{\ell}|^2}{4\Gamma} \left[ \frac{1}{1+x^2} (1 - |\cos \theta|^2 - |\sin \theta e^{-i\phi}|^2) + i \frac{x}{1+x^2} (\cos \theta - \cos \theta^*) + \frac{1}{1-y^2} (1 + |\cos \theta|^2 + |\sin \theta e^{-i\phi}|^2) + \frac{y}{1-y^2} (\cos \theta + \cos \theta^*) \right], \quad (55)$$

$$N^- = \frac{|\bar{A}_{\ell}|^2}{4\Gamma} \left[ \frac{1}{1+x^2} (1 - |\cos \theta|^2 - |\sin \theta e^{i\phi}|^2) + i \frac{x}{1+x^2} (\cos \theta - \cos \theta^*) + \frac{1}{1-y^2} (1 + |\cos \theta|^2 + |\sin \theta e^{i\phi}|^2) - \frac{y}{1-y^2} (\cos \theta + \cos \theta^*) \right]. \quad (56)$$

These are the exact expressions for  $N^+$  and  $N^-$ , obtained without assuming  $CPT$  invariance. When  $CPT$  invariance is assumed, the above equations simplify to

$$N^+ = \frac{|A_{\ell}|^2}{4\Gamma} \left[ (1 - |e^{-i\phi}|^2) \frac{1}{1+x^2} + (1 + |e^{-i\phi}|^2) \frac{1}{1-y^2} \right], \quad (57)$$

$$N^- = \frac{|\bar{A}_{\ell}|^2}{4\Gamma} \left[ (1 - |e^{i\phi}|^2) \frac{1}{1+x^2} + (1 + |e^{i\phi}|^2) \frac{1}{1-y^2} \right]. \quad (58)$$

Using  $\chi = (x^2 + y^2)/2(1 + x^2)$  which is a mixing parameter described later, the inclusive lepton yields from the  $Y(4S)$  decay is obtained as

$$N^+ = \frac{|A_{\ell}|^2}{\Gamma(1-y^2)} [1 + (|e^{-i\phi}|^2 - 1)\chi], \quad (59)$$

$$N^- = \frac{|\bar{A}_{\ell}|^2}{\Gamma(1-y^2)} [1 + (|e^{i\phi}|^2 - 1)\chi]. \quad (60)$$

One notes here that there is an asymmetry in  $N^+$  and  $N^-$  if  $|e^{-i\phi}|^2 \neq |e^{i\phi}|^2$ . Therefore,  $Y(4S)$  decay into single lepton final states can also give rise to an asymmetry which may give a signature of  $CP$  violation. The single lepton charge asymmetry can be obtained from the above equations as

$$A_{\text{sym}}^{\ell} = \frac{N^+ - N^-}{N^+ + N^-} = \frac{(|e^{-i\phi}|^2 - |e^{i\phi}|^2)\chi}{2 + (|e^{-i\phi}|^2 + |e^{i\phi}|^2 - 2)\chi} \approx \chi A_{\text{sym}}^{\ell\ell}. \quad (61)$$

Here, we assume  $|A_{\ell}|^2 = |\bar{A}_{\ell}|^2$  as in Eq. (43). It is to be noted that the single lepton method is more useful in detecting  $CP$  violation for larger  $\chi$  [9]. The most recent result of  $\chi = 0.149 \pm 0.031$  (CLEO) [10] is rather large for an effective utilization of this method.

### E. Time evolution of opposite sign dileptons

We now calculate the joint decay rates to opposite-sign dilepton final states and discuss their time evolution. Let us first consider the case where

$$f_a = \ell^+ X^-, \quad f_b = \ell^- X^+,$$

then

$$A_a = \langle B^0 | \ell^+ X^- \rangle = A_{\ell}, \quad \bar{A}_a = \langle \bar{B}^0 | \ell^+ X^- \rangle = 0,$$

$$A_b = \langle B^0 | \ell^- X^+ \rangle = 0, \quad \bar{A}_b = \langle \bar{B}^0 | \ell^- X^+ \rangle = \bar{A}_{\ell}.$$

The joint decay rate is obtained using Eq. (27) as

$$\begin{aligned} \Gamma_{Y(4S) \rightarrow \ell^+ \ell^-}(t_1, t_2) &= \frac{1}{2} e^{-\Gamma(t_1+t_2)} |A_{\ell} \bar{A}_{\ell}|^2 (|\cos[\Delta\mu(t_1-t_2)/2]|^2 \\ &+ |\cos \theta \sin[\Delta\mu(t_1-t_2)/2]|^2 \\ &- 2 \text{Im}\{\cos \theta \sin[\Delta\mu(t_1-t_2)/2] \\ &\times \cos[\Delta\mu^*(t_1-t_2)/2]\}). \end{aligned} \quad (62)$$

After simplifying and using the values of  $\Delta\mu$  and  $\Delta\mu^*$  in terms of  $\Delta m$  and  $\Delta\Gamma$ , the joint decay rate in this particular case is

$$\begin{aligned} \Gamma_{Y(4S) \rightarrow \ell^+ \ell^-}(t_1, t_2) &= \frac{1}{4} e^{-\Gamma(t_1+t_2)} |A_{\ell} \bar{A}_{\ell}|^2 (\cosh[\Delta\Gamma(t_1-t_2)/2] \\ &+ \cos[\Delta m(t_1-t_2)] + |\cos \theta|^2 \{ \cosh[\Delta\Gamma(t_1-t_2)/2] \\ &- \cos[\Delta m(t_1-t_2)] \} + 2 \text{Re}(\cos \theta) \sinh[\Delta\Gamma(t_1-t_2)/2] \\ &- 2 \text{Im}(\cos \theta) \sin[\Delta m(t_1-t_2)]). \end{aligned} \quad (63)$$

Next, we consider the case where

$$f_a = \ell^- X^+, \quad f_b = \ell^+ X^-,$$

then

$$A_a = \langle B^0 | \ell^- X^+ \rangle = 0, \quad \bar{A}_a = \langle \bar{B}^0 | \ell^- X^+ \rangle = \bar{A}_\ell$$

$$A_b = \langle B^0 | \ell^+ X^- \rangle = A_\ell, \quad \bar{A}_b = \langle \bar{B}^0 | \ell^+ X^- \rangle = 0.$$

Exactly in the same way as in the  $\ell^+(t_1)\ell^-(t_2)$  case, the joint decay rate  $\Gamma_{Y(4S) \rightarrow \ell^- \ell^+}$  is obtained as

$$\begin{aligned} \Gamma_{Y(4S) \rightarrow \ell^- \ell^+}(t_1, t_2) &= \frac{1}{2} e^{-\Gamma(t_1+t_2)} |A_\ell \bar{A}_\ell|^2 \times (|\cos[\Delta\mu(t_1-t_2)/2]|^2 + |\cos\theta \sin[\Delta\mu(t_1-t_2)/2]|^2 \\ &\quad + 2 \operatorname{Im}\{\cos\theta \sin[\Delta\mu(t_1-t_2)/2] \cos[\Delta\mu^*(t_1-t_2)/2]\}) \end{aligned} \quad (64)$$

$$\begin{aligned} &= \frac{1}{4} e^{-\Gamma(t_1+t_2)} |A_\ell \bar{A}_\ell|^2 \times (\cosh[\Delta\Gamma(t_1-t_2)/2] + \cos[\Delta m(t_1-t_2)]) \\ &\quad + |\cos\theta|^2 \{\cosh[\Delta\Gamma(t_1-t_2)/2] - \cos[\Delta m(t_1-t_2)]\} - 2 \operatorname{Re}(\cos\theta) \sinh[\Delta\Gamma(t_1-t_2)/2] \\ &\quad + 2 \operatorname{Im}(\cos\theta) \sin[\Delta m(t_1-t_2)], \end{aligned} \quad (65)$$

In the following, we always define the decay time of  $\ell^+$  to be  $t_1$  and that of  $\ell^-$  to be  $t_2$ . Integrating over  $t_+ = t_1 + t_2$ , the observed joint decay rate as a function of  $\Delta t$  is given as

$$\begin{aligned} \Gamma_{Y(4S) \rightarrow \ell^+ \ell^-}(\Delta t) &= \frac{1}{2\Gamma} e^{-\Gamma|\Delta t|} |A_\ell \bar{A}_\ell|^2 \times [\cosh(\Delta\Gamma\Delta t/2) + \cos(\Delta m\Delta t) \\ &\quad + |\cos\theta|^2 \{\cosh(\Delta\Gamma\Delta t/2) - \cos(\Delta m\Delta t)\} + 2 \operatorname{Re}(\cos\theta) \sinh(\Delta\Gamma\Delta t/2) - 2 \operatorname{Im}(\cos\theta) \sin(\Delta m\Delta t)]. \end{aligned} \quad (66)$$

The presence of  $\cos\theta$  terms in Eq. (66) indicates the  $CPT$  violation and it can best be seen if we define an asymmetry

$$A_{\text{sym}}^{+-}(\Delta t) = \frac{\Gamma_{Y(4S) \rightarrow \ell^+ \ell^-}(\Delta t) - \Gamma_{Y(4S) \rightarrow \ell^+ \ell^-}(-\Delta t)}{\Gamma_{Y(4S) \rightarrow \ell^+ \ell^-}(\Delta t) + \Gamma_{Y(4S) \rightarrow \ell^+ \ell^-}(-\Delta t)}. \quad (67)$$

Substituting the expressions of Eq. (66) it can be expressed as

$$A_{\text{sym}}^{+-}(\Delta t) = \frac{2 \operatorname{Re}(\cos\theta) \sinh(\Delta\Gamma\Delta t/2) - 2 \operatorname{Im}(\cos\theta) \sin(\Delta m\Delta t)}{\cosh(\Delta\Gamma\Delta t/2) + \cos(\Delta m\Delta t) + |\cos\theta|^2 [\cosh(\Delta\Gamma\Delta t/2) - \cos(\Delta m\Delta t)]}. \quad (68)$$

It is natural to assume that  $CPT$ -violating effect is small so that we can set  $|\cot\theta| \ll 1$  and  $\cos\theta \approx \cot\theta$ , and keep only  $O(\cot\theta)$  terms. Then Eq. (68) becomes

$$A_{\text{sym}}^{+-}(\Delta t) = \frac{2 \operatorname{Re}(\cot\theta) \sinh(\Delta\Gamma\Delta t/2) - 2 \operatorname{Im}(\cot\theta) \sin(\Delta m\Delta t)}{\cosh(\Delta\Gamma\Delta t/2) + \cos(\Delta m\Delta t)}. \quad (69)$$

If one puts  $\Delta\Gamma = 0$  then one gets

$$A_{\text{sym}}^{+-}(\Delta t) = \frac{-2 \operatorname{Im}(\cot\theta) \sin(\Delta m\Delta t)}{1 + \cos(\Delta m\Delta t)}. \quad (70)$$

It should be noted that for a small range of  $\Delta m\Delta t$  near  $(2n+1)\pi$  where  $n$  is an integer, Eq. (70) is a poor approximation to Eq. (68). If  $CPT$  is conserved then the decay rates of opposite sign dileptons are reduced to

$$\Gamma_{Y(4S) \rightarrow \ell^+ \ell^-}(\Delta t) = \frac{|A_\ell \bar{A}_\ell|^2}{4} e^{-\Gamma|\Delta t|} [\cosh(\Delta\Gamma\Delta t/2) + \cos(\Delta m\Delta t)] = \Gamma_{Y(4S) \rightarrow \ell^+ \ell^-}(-\Delta t), \quad (71)$$

and  $A_{\text{sym}}^{+-}$  obviously becomes zero.

Integrating Eq. (66) over  $\Delta t$ , the time-integrated number of  $\ell^+ \ell^-$  events is given as

$$N^{+-} = \frac{|A_{\rho}\bar{A}_{\rho}|^2}{2\Gamma^2} \left[ \frac{2+x^2-y^2}{(1+x^2)(1-y^2)} + |\cos \theta|^2 \frac{x^2+y^2}{(1+x^2)(1-y^2)} \right]. \quad (72)$$

From Eqs. (35), (40), and (72), the observable mixing parameter  $\chi$  is written as

$$\chi \equiv \frac{N^{++} + N^{--}}{N^{+-} + N^{++} + N^{--}} \quad (73)$$

$$= \frac{|\sin \theta|^2 (|e^{-i\phi}|^2 + |e^{i\phi}|^2)(x^2 + y^2)}{2(2+x^2-y^2) + 2|\cos \theta|^2(x^2+y^2) + |\sin \theta|^2 (|e^{-i\phi}|^2 + |e^{i\phi}|^2)(x^2+y^2)} \quad (74)$$

$$= \frac{(|e^{-i\phi}|^2 + |e^{i\phi}|^2)(x^2 + y^2)}{2(2+x^2-y^2)|1 + \cot^2 \theta| + 2|\cot \theta|^2(x^2+y^2) + (|e^{-i\phi}|^2 + |e^{i\phi}|^2)(x^2+y^2)}. \quad (75)$$

Here, we assume  $|A_{\rho}|^2 = |\bar{A}_{\rho}|^2$  as in Eq. (43). If  $CPT$  is conserved and the charge asymmetry of the  $B^0\bar{B}^0$  mixing is small ( $|e^{\pm i\phi}|^2 \cong 1 \mp 2 \operatorname{Im}(\phi)$ ), the expression for  $\chi$  reduces to the standard one

$$\chi = \frac{1}{2} \frac{x^2 + y^2}{1 + x^2}. \quad (76)$$

### III. SIMULATION STUDIES

#### A. Event generation

We used the  $QQ$  event generator program (version 8.08) which was developed by the CLEO group to generate  $Y(4S)$  and  $q\bar{q}$  continuum events.  $Y(4S)$  decays into  $B^0\bar{B}^0$  and  $B^+B^-$  with equal branching ratios and all  $B^0$ ,  $\bar{B}^0$ , and  $B^{\pm}$  decay generically with a default  $QQ$  decay table tuned to the CLEO data. The  $B^0\bar{B}^0$  mixing was included with  $x_d = 0.66$  and  $\Delta\Gamma$  was assumed to be 0. The value of  $x_d = 0.66$  was given in a default  $QQ$  decay table based on the CLEO measurements [10], and not the most recent result. However, this does not affect the outcome of our analysis. We set the  $CP$ -violation parameter  $\operatorname{Im}(\phi)$  to 0. The  $CPT$ -violation parameter  $\cot \theta$  was set to 0 except for the opposite sign dilepton study.  $10^6$  events were generated each for  $Y(4S)$  and continuum events and analyzed. The obtained number of events are normalized according to the cross section ratios 1.15 and 2.8 nb for  $Y(4S)$  and continuum, respectively.  $10^6$   $Y(4S)$  events corresponds to the integrated luminosity of  $0.87 \text{ fb}^{-1}$ .

#### B. Simulation of the BELLE detector

Figure 1 shows the BELLE detector, which the detector simulation program in this paper is based on. The expected performance of the detector is summarized in Table I.

We used a fast detector simulator (FSIM) program in which the detector response were parametrized based on the results of detector research an development or GEANT full

detector simulation studies. The simulation parameters relevant to this study are described in the following.

#### 1. Charged particle tracking

The detection and reconstruction of charged particles are done by the SVD (silicon vertex detector) and CDC (central drift chamber). The charged particle tracking efficiency was parametrized as a function of particle type, minimum detectable momentum ( $p_{\min}$ ), total momentum ( $p$ ), and polar angle of the particle ( $\theta$ ) based on the GEANT full detector simulation study. The SVD and CDC cover the polar angle  $17^\circ < \theta < 150^\circ$ . The track is represented by a helix with the following five parameters:  $p_t$ , the transverse momentum with respect to the beam axis ( $=z$  axis);  $d_0$ , the closest distance from the  $z$  axis of the track helix;  $z_0$ , the  $z$  position of the closest point to the  $z$  axis of the track helix;  $\phi_0$ , the azimuthal angle of track direction at the closest point to  $z$  axis;  $\theta$ , the polar angle of track direction.

These track-helix resolutions for the combined CDC + SVD tracking system are parametrized as a function of the particle momentum, velocity ( $\beta$ ), and  $\theta$  as

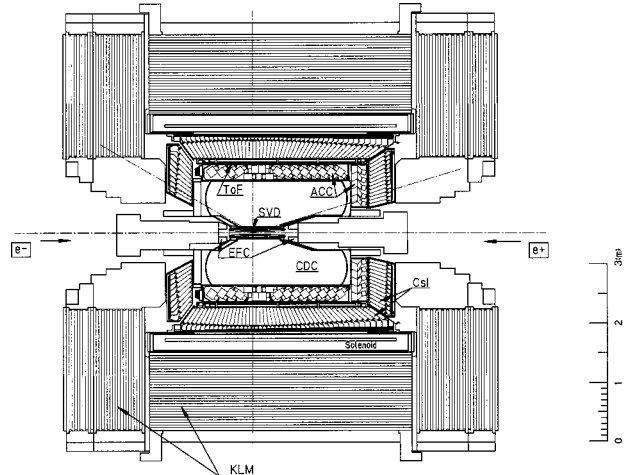


FIG. 1. BELLE detector used in this simulation study.

TABLE I. Performance parameters of the BELLE detector used in the simulation.

Detector	Type	Configuration	Performance
Beam pipe	Beryllium double wall double sided	cylindrical, $r=2.3$ cm 0.5 mm Be/2 mm He/0.5 mm Be 300- $\mu$ m thick, 4 layers $r=2.7-5.8$ cm	Helium gas cooled $\sigma_{r\phi} \leq 10$ $\mu$ m $\sigma_z = 7-40$ $\mu$ m
SVD	Si strip small cell	length=22-34 cm anode: 52 layers cathode: 3 layers	$\sigma_{\Delta z} \sim 80$ $\mu$ m $\sigma_{r\phi} = 130$ $\mu$ m
CDC	drift chamber	$r=8.5-90$ cm $-77 \leq z \leq 160$ cm	$\sigma_z = 200-1400$ $\mu$ m $\sigma_{dE/dx} = 6\%$
PID	silica aerogel $n \approx 1.01$	$\sim 12 \times 12 \times 12$ cm <sup>3</sup> blocks 960 barrel/268 endcap FM-PMT readout	$N_{p.e.} \geq 6$ K/ $\pi$ $1.2 < p < 3.5$ GeV/c
TOF	scintillator	128 $\phi$ segmentation $r=120$ cm, 3-m long towered structure	$\sigma_t = 100$ ps K/ $\pi$ up to 1.2 GeV/c $\sigma_E/E =$
ECL	cesium iodide crystal (CsI)	$\sim 5.5 \times 5.5 \times 30$ cm <sup>3</sup> crystals barrel: $r=125-162$ cm endcap: $z=-102$ and 196 cm	$0.67\% / \sqrt{E} \oplus 1.8\%$ $\sigma_{pos} = 0.5$ cm/ $\sqrt{E}$ $E$ in GeV
MAGNET	super- conducting	inner radius = 170 cm	B = 1.5 T
KLM	resistive plate counter	14 layers (5 cm Fe + 4 cm gap) two RPCs in each gap $\theta$ and $\phi$ strips	$\Delta\phi = \Delta\theta = 30$ mr for $K_L$ $\sigma_t = 1$ ns 1% hadron fakes

$$\frac{\sigma_{p_t}}{p_t} \approx 0.11 p_t \oplus \frac{0.20}{\beta} \% \quad (\theta = 90^\circ), \quad (77)$$

$$\sigma_{d_0} = 19 \oplus \frac{31}{p\beta \sin^{3/2} \theta} \mu\text{m}, \quad (78)$$

$$\sigma_{z_0} = (13 + 67 \cos^2 \theta) \oplus \frac{30}{p\beta \sin^{5/2} \theta} \mu\text{m}, \quad (79)$$

$$\sigma_{\phi_0} = 0.47 \oplus \frac{1.16}{p\beta \sin^{3/2} \theta} \text{mr}, \quad (80)$$

$$\sigma_{\cot \theta} = (0.34 + 1.92 \cos^2 \theta) \oplus \frac{1.14}{p\beta \sin^{5/2} \theta} \times 10^{-3}. \quad (81)$$

## 2. Lepton identification

*Electrons.* The electron identification is provided by comparing the energy deposit in the CsI calorimeter and the measured momenta of the corresponding track. The electron identification efficiency is

$$\text{eff} = 0.0 \quad (E < 0.5 \text{ GeV}), \quad (82)$$

$$= 0.9 \quad (0.5 \leq E < 1.0 \text{ GeV}), \quad (83)$$

$$= 0.95 \quad (1.0 \text{ GeV} \leq E). \quad (84)$$

The CsI calorimeter covers polar angle region  $17^\circ < \theta < 150^\circ$ . The probability for misidentifying a hadron as an electron depends on the sign of the particle's charge and its momentum as shown in Fig. 2. These numbers are based on our research and development results.

The  $dE/dx$  information from the CDC can also provide the electron identification which is particularly useful in the low momentum region. However, we only used the CsI calorimeter and did not use the  $dE/dx$  information in this analysis.

*Muons.* The muon identification is provided by the KLM

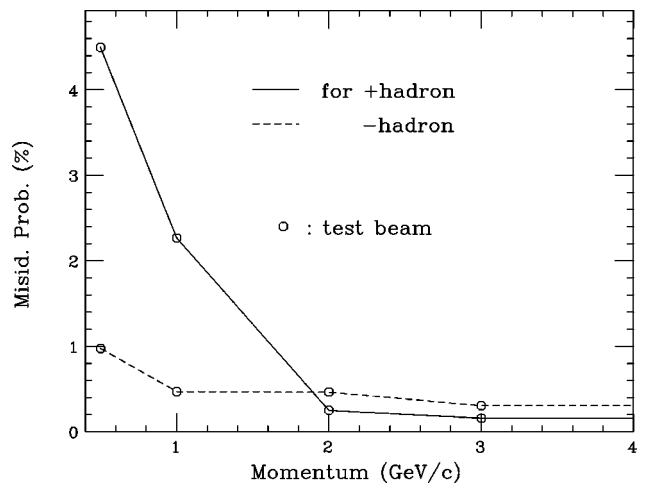


FIG. 2. Probability for misidentifying a hadron as an electron in the CsI.

TABLE II. Contribution to  $z$ -vertex resolution from various sources.

	$\sigma_{\text{beam}}$	$\sigma_{\text{flight}}$	$\sigma_{\text{meas}}$	total
electron	82 $\mu\text{m}$	28 $\mu\text{m}$	93 $\mu\text{m}$	127 $\mu\text{m}$
muon	61 $\mu\text{m}$	23 $\mu\text{m}$	51 $\mu\text{m}$	83 $\mu\text{m}$

which consists of 14 layers of 5-cm-thick iron plates and RPC (resistive plate counter) planes. The muon identification efficiency is 90% for  $p \geq 1.2$  GeV/ $c$  and zero for lower momentum over the  $30^\circ \leq \theta \leq 140^\circ$  angular region. This momentum cut approximately corresponds to the energy loss of a muon in 1-m-thick iron. The hadron punch-through rate is 1%. These are crude approximations of full-simulation results.

### 3. Lepton $Z$ -vertex determination

In this analysis, we used a simple method for the determination of the  $z$ -vertex position of a lepton. We defined the  $z$  position of closest point to the  $z$  axis of the lepton track (i.e.,  $z_0$  of the helix parameter of the lepton track) as the  $z$  position of the lepton vertex. This method assumes the decay point of  $B$  mesons to be on the  $z$  axis, and therefore neglects a beam spread and a flight path before decay in  $x$ - $y$  directions. These contribute to the error of the  $z$ -vertex measurement in addition to the detector resolution and the multiple scattering effect. We examined the contribution of each source to the  $z$ -vertex measurement error for primary leptons by comparing the  $z$ -vertex resolutions with and without the beam spread and detector effect. Table II summarizes the result. The beam spread is assumed to be  $\sigma_x = 110$   $\mu\text{m}$ ,  $\sigma_y = 3$   $\mu\text{m}$ , and  $\sigma_z = 0.6$  cm in the simulation. The contribution from the beam spread is similar to that from the detector effect. The poorer resolution for electrons than muons is due to the larger forward and backward acceptance coverage of the electron detection. In this method of determining the vertex  $z$  position, forward and backward tracks suffer a larger effect than the central track. An extended detection coverage of electrons for lower momentum than the muon is also a source of worse  $\sigma_{\text{meas}}$  because of the larger multiple scattering effect.

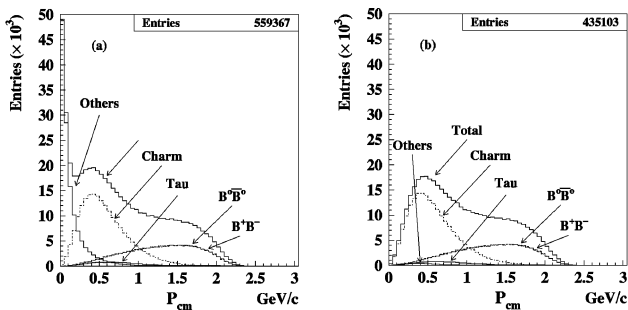


FIG. 3. Lepton momentum spectra in the c.m. frame for the generated leptons from  $Y(4S)$  for various sources. All the generated leptons are included (no acceptance cut is applied): (a) for electrons and (b) for muons.

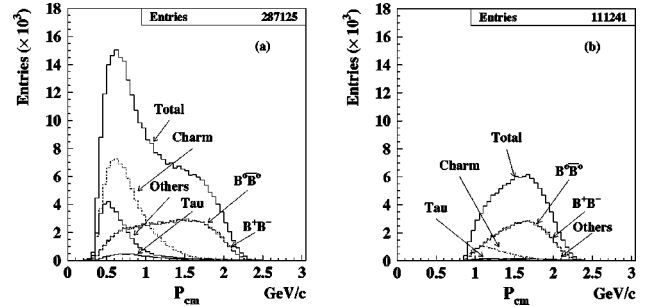


FIG. 4. Lepton momentum spectra in the c.m. frame for the detected leptons from  $Y(4S)$  for various sources: (a) for electrons and (b) for muons.

### C. Lepton sources and c.m. momentum distributions

Since the leptons are originated from various sources in the  $e^+e^-$  collisions at  $Y(4S)$ , we first examined the sources and the c.m. momentum ( $P_{\text{c.m.}}$ ) distributions of the single leptons. We categorized the source of leptons into the following six types: (a) primary decay from  $B^0$  and  $\bar{B}^0$  mesons; (b) primary decay from  $B^+$  and  $B^-$  mesons; (c) leptons from charmed mesons (neutral and charged  $D$ ,  $D^*$ ,  $D_s^*$  only, charmed baryons are not included); (d) leptons from tau leptons; (e) leptons from other hadrons; (f) misidentified hadrons (fake leptons).

In order to understand the behavior of the detected leptons from different sources, we examined the c.m. momentum distributions of leptons in two cases: for all the generated leptons without detector effects and the identified leptons by the detectors mentioned in the previous section. Figures 3 and 4 show the c.m. momentum spectra of the generated leptons for various sources from  $Y(4S)$  and the continuum events. Here, the number of events are for  $10^6$  generated events in both  $Y(4S)$  and continuum cases. Figures 5 and 6 show the c.m. momentum spectra of the identified leptons. As is well known, primary leptons from neutral and charged  $B$  mesons are peaked at higher momentum ( $P_{\text{c.m.}} \sim 1.5$  GeV), while leptons from all other sources, whose main contribution comes from charm decays, are peaked at low momentum. The distributions for muons are similar to those for electrons except that low momentum components from hadrons are only present in the electron. As commonly adopted,

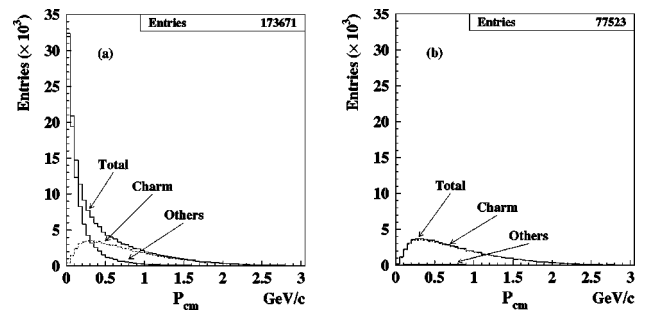


FIG. 5. Lepton momentum spectra in the c.m. frame for the generated leptons from the continuum events for various sources. All the generated leptons are included (no acceptance cut is applied): (a) for electrons and (b) for muons.

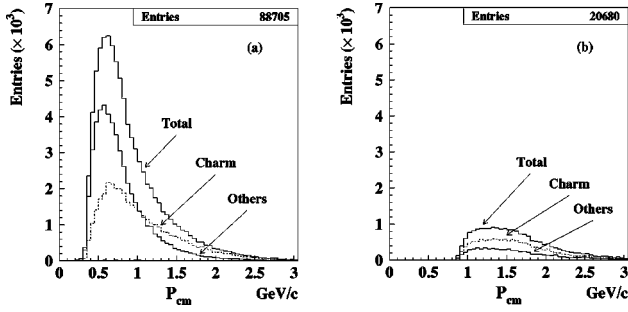


FIG. 6. Lepton momentum spectra in the c.m. frame for the detected leptons from the continuum events for various sources: (a) for electrons and (b) for muons.

the cut on the lepton momentum effectively reduces the fraction of background.

#### D. Analysis of same-sign dilepton events

##### 1. Event selection

In the events with two or more identified leptons, the same-sign dileptons are selected and classified into three categories: SS-1, both are primary leptons (i.e., from neutral  $B$  mesons only); SS-2, both are leptons, but at least one is not a primary lepton; SS-3, at least one is a fake lepton. Category SS-1 is the signals and categories SS-2 and SS-3 are the backgrounds. When more than two leptons are found in one event, all pairs of leptons are taken. As expected from the single lepton distributions, events in categories SS-2 and SS-3 mainly consist of one high and one low momentum lepton pair. This implies a simultaneous cut on both lepton momenta eliminates a large fraction of these categories. Figure 7 shows the same-sign dilepton yield for each source as a function of lepton momentum cut value, where we required that both lepton momenta were above the cut value. As expected, backgrounds fall rapidly for low momentum cut values, i.e., ( $<1.5$  GeV), while signals fall smoothly.

##### 2. Sensitivity to charge asymmetry

Figure 8 shows the expected statistical errors of the asymmetry measurement as a function of lepton momentum cut

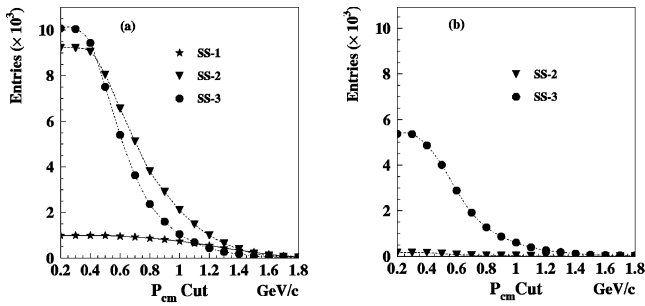


FIG. 7. Same-sign dilepton yield vs lepton momentum cut in c.m. frame with luminosity of  $0.87 \text{ fb}^{-1}$ : (a) from  $Y(4S)$  and (b) from continuum. Electrons and muons are summed together. Same-sign dileptons are classified into three categories which are described in the text.

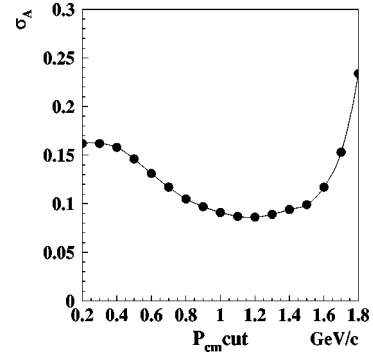


FIG. 8. Expected statistical errors of the charge asymmetry measurement for the same-sign dileptons as a function of lepton momentum cut with the luminosity corresponding to  $0.87 \text{ fb}^{-1}$ .

with the luminosity corresponding to  $0.87 \text{ fb}^{-1}$ . In the calculation, we followed a general formula for the statistical error estimation

$$\sigma_A^2 = \frac{1}{S^2} [(1-A^2)N + 2A(A-X)B + (A-X)^2\sigma_B^2 + B^2\sigma_X^2], \quad (85)$$

where  $A$  is the signal symmetry,  $S$  the number of signal events,  $B$  the total number of background events,  $X$  the asymmetry of the background,  $N$  the total number of events ( $=S+B$ ). Assuming no asymmetry in background ( $X=0$ ) and neglecting its error ( $\sigma_X=0$ ), the formula reduces for small signal asymmetry ( $A^2 \ll 1$ ) to

$$\sigma_A \approx \sqrt{\frac{1+B/S}{S}}. \quad (86)$$

The optimum cut is  $\sim 1.2 \text{ GeV}/c$  and we expect to get  $\sigma_A \sim 0.008$  with a luminosity of  $100 \text{ fb}^{-1}$ .

With the above momentum cut the signal events are reduced to about half, but still  $N/S$  is  $\sim 3$ . Therefore, it is possible to improve the sensitivity by combining with other effective cuts to further reduce the backgrounds while keeping the same or more signal events. As seen in Fig. 7, the dominant background is category SS-2 from  $Y(4S)$  where one is a primary lepton from  $B$  meson and the other comes from secondary charm decay.

##### 3. $\Delta z$ cut

As described in the previous section, the proper time distribution of the same-sign dilepton events is given by Eqs. (34) and (39). The time evolution for  $\ell^+\ell^+$  and  $\ell^-\ell^-$  are exactly the same. The population is zero at  $|t_1 - t_2| = 0$  and has a peak  $|t_1 - t_2| \sim 0.6\pi\tau_B$ . Since  $\beta\gamma c\tau_B \sim 0.2 \text{ mm}$  with  $8 \times 3.5 \text{ GeV}$  KEK  $B$  factory, the peak corresponds to  $\Delta z \sim 400 \mu\text{m}$ , where  $\Delta z$  is the difference of two lepton vertices along the  $z$  axis. On the other hand, for backgrounds from any sources we expect exponential distribution in  $\Delta z$  which peaks at  $\Delta z = 0$ . Therefore, cut on  $\Delta z$  would enhance  $S/N$  ratio and improve the sensitivity.

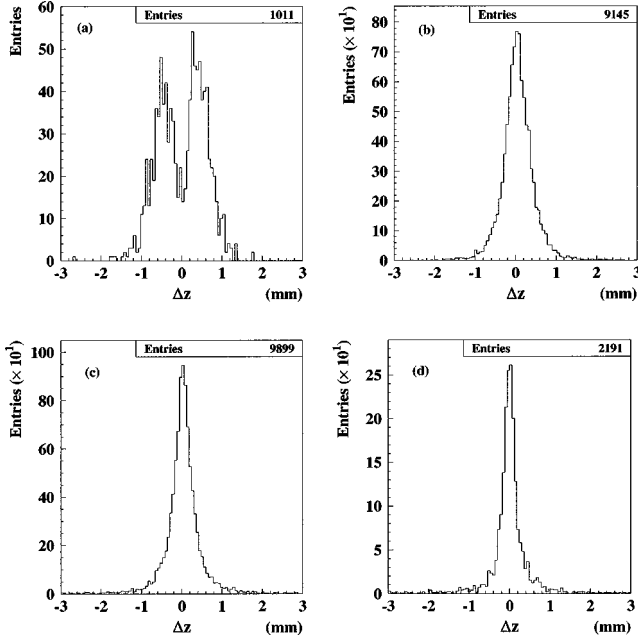


FIG. 9.  $\Delta z$  distributions for the same-sign dileptons for various categories. No lepton momentum cut is applied.  $ee$ ,  $\mu\mu$ , and  $e\mu$  events are summed up. (a) For signals, (b) for category SS-2 from  $Y(4S)$ , (c) for category SS-3 from  $Y(4S)$ , and (d) category SS-2 and SS-3 from continuum.

Figure 9 shows  $\Delta z$  for the same-sign dileptons for various categories. As expected, the distribution for category 1 shows a dip at  $\Delta z=0$  and has peaks  $|\Delta z| \sim 400 \mu\text{m}$ , whereas those for backgrounds peak at  $\Delta z=0$ .

We applied cuts on lepton momenta and  $\Delta z$  trying to find the optimal cuts. Figure 10 shows the expected statistical errors of the asymmetry measurement as a function of lepton momentum cut for various  $\Delta z$  cut values with the luminosity corresponding to  $0.87 \text{ fb}^{-1}$ . An optimum cut is found with  $\Delta z$  cut of 0.3 mm and  $P_{\text{c.m.}}$  cut of 1.1  $\text{GeV}/c$ . The statistical error is improved by  $\sim 20\%$  compared with that of  $P_{\text{c.m.}}$  cut alone and we expect to get  $\sigma_A \sim 0.0066$  with a luminosity of  $100 \text{ fb}^{-1}$ .

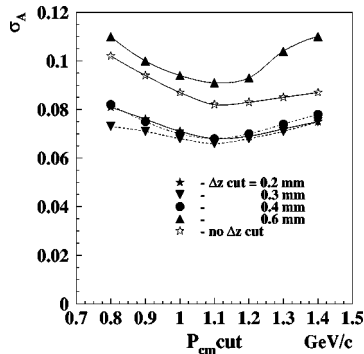


FIG. 10. Expected statistical errors of the asymmetry measurement as a function of lepton momentum cut for various  $\Delta z$  cut values with the luminosity corresponding to  $0.87 \text{ fb}^{-1}$ .  $ee$ ,  $\mu\mu$ , and  $e\mu$  events are summed up.

TABLE III. Number of single leptons with lepton c.m. momentum cut at 1.1  $\text{GeV}/c$  for the luminosity of  $0.87 \text{ fb}^{-1}$ .

	lepton source	number of leptons
signal	primary leptons from $B^0$ and $\bar{B}^0$	$93.7 \times 10^3$
	primary leptons from $B^\pm$	$93.7 \times 10^3$
background	other leptons from $Y(4S)$	$30.8 \times 10^3$
	leptons from continuum events	$97.4 \times 10^3$
total background		$221.9 \times 10^3$

### E. Analysis of single lepton events

As described in the previous section, the charge asymmetry can also be measured by the single leptons. The magnitude of the asymmetry is diluted by factor  $\chi_d$ , but statistical sensitivity can be better because of the much larger number of samples [9].

We applied cuts on lepton c.m. momenta at 1.1  $\text{GeV}/c$  which minimized the factor  $\sqrt{(1+B/S)/S}$ , where  $S$  is the number of primary leptons from  $B^0$  and  $\bar{B}^0$  [source type (a)] and  $B$  is the number of background leptons from all other sources. The result is listed in Table III. The primary leptons from  $B^\pm$  cannot be distinguished from those from  $B^0$  and  $\bar{B}^0$  and contribute to the background the same amount as the signals. Using Eq. (86) we obtained the statistical error of asymmetry  $\sigma_{A_\ell} = 0.006$  for the integrated luminosity of  $0.87 \text{ fb}^{-1}$ , which corresponds to  $\sigma_{A_{\ell\ell}} = \sigma_{A_\ell} / \chi_d = 0.04$ . Thus, as expected, the single lepton asymmetry measurement can provide better statistical sensitivity than the same-sign dilepton case ( $\sigma_{A_{\ell\ell}} = 0.066$ ). Combining the two measurements, we obtained the sensitivity  $\sigma_{A_{\ell\ell}} = 0.034(0.0034)$  for an integrated luminosity of  $0.87(100) \text{ fb}^{-1}$ .

### F. Analysis of opposite-sign dilepton events

#### 1. Event selection

Events containing opposite-sign dileptons are selected and classified into five categories: OS-1, both are primary leptons from  $B^0\bar{B}^0$ ; OS-2, both are primary leptons from  $B^+B^-$ ; OS-3, both are leptons from charmed mesons  $c$  and  $\bar{c}$ ; OS-4, others but no fake lepton; OS-5, at least one is a fake lepton (fake). Only the events in category OS-1 constitute the signal we are interested in. However, since the events in the category OS-2 have identical signature and we cannot separate them, we must treat the events in these two categories together. Others are backgrounds. Again, multiple pairs of leptons found in one event are included. Events in the category OS-4 and OS-5 (major backgrounds) mainly consist of one high and one low momentum lepton pair as expected from the single lepton momentum distribution. A simultaneous cut on both lepton momenta successfully eliminates a large fraction of these categories.

Figure 11 shows the yield as a function of  $P_{\text{c.m.}}$  cut for each category of opposite-sign dilepton events. We optimized the cut value by minimizing the factor  $\sqrt{(1+B/S)/S}$ ,

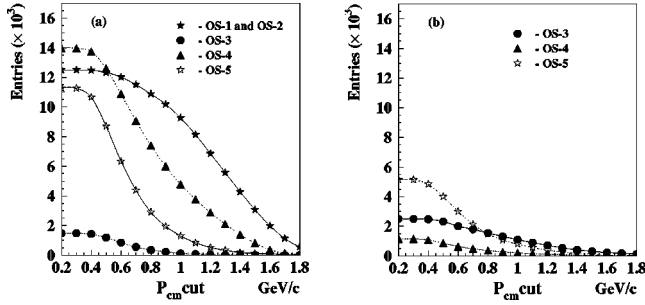


FIG. 11. Opposite-sign dilepton yield vs lepton momentum cut in c.m. frame with luminosity of  $0.87 \text{ fb}^{-1}$ . (a) From  $Y(4S)$  and (b) from continuum. Electrons and muons are summed together.

where  $S$  and  $B$  are the number of signal events (categories OS-1 and OS-2) and those of other background events, respectively. We used the  $1.0 \text{ GeV}/c$  cut for the analysis.

## 2. Proper-time distribution and determination of $\text{Im}(\cot \theta)$

Figure 12 shows the distributions of the proper-time difference for the opposite-sign dileptons that passed the  $P_{\text{c.m.}}$  cut in each category. The proper-time difference  $\Delta\tau (= \Delta t / \tau_B)$  is calculated from the  $z$  vertices using the following expression:

$$\Delta\tau = \tau_1 - \tau_2 = \frac{t_1}{\tau_B} - \frac{t_2}{\tau_B} = \frac{z_1}{c\beta\gamma\tau_B} - \frac{z_2}{c\beta\gamma\tau_B} = \frac{\Delta z}{c\beta\gamma\tau_B}, \quad (87)$$

where  $z_i$  = the measured  $z$  vertex of the  $i$ th lepton,  $\beta\gamma$  = the Lorentz boost factor of the  $e^+e^-$  c.m. system, and  $\tau_B = B^0$

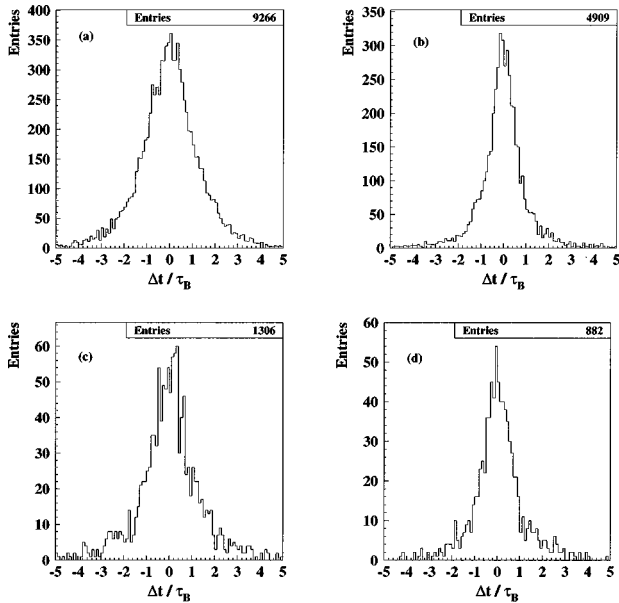


FIG. 12. Proper time distributions for the opposite-sign dileptons from various categories. Lepton momentum cut ( $P_{\text{c.m.}} \geq 1.0 \text{ GeV}/c$ ) is applied.  $ee$ ,  $\mu\mu$ , and  $e\mu$  events are summed up. (a) For primary leptons from  $B^0$  and  $B^\pm$  (category OS-1 and OS-2), (b) for category OS-3 and OS-4 (summed) from  $Y(4S)$ , (c) for category OS-5 from  $Y(4S)$ , and (d) all leptons from continuum.

lifetime. We call the positively charged lepton lepton-1 and the negatively charged one as lepton-2.

It is not possible to distinguish the primary leptons coming from neutral and charged  $B$ 's. On the other hand, the time evolutions of the neutral and charged  $B$  mesons are known exactly. So the data containing both neutral and charged  $B$  mesons can be fit to a theoretical expression that also contains both  $B^0\bar{B}^0$  and  $B^+B^-$ . Other backgrounds are assumed to be subtracted using Monte Carlo or continuum data taken below  $Y(4S)$ , although the errors of the background statistics must be taken into account correctly. The theoretical function which expresses the proper-time evolution is given by

$$f(\Delta t') \propto e^{-\Gamma|\Delta t'|} [1 + \cos x_d(\Delta t' / \tau_B) - 2 \text{Im}(\cot \theta) \sin x_d(\Delta t' / \tau_B)] + 2e^{-\Gamma|\Delta t'|}. \quad (88)$$

Here the first and second terms are from  $B^0\bar{B}^0$  and  $B^+B^-$  contributions, respectively. The observed proper time difference distribution must be modified by taking into account the experimental resolution for the proper time:

$$F(\Delta t) = \int g(\Delta t - \Delta t') f(\Delta t') d(\Delta t'), \quad (89)$$

where  $g(\Delta t - \Delta t')$  is the resolution function that is determined by fitting the Monte Carlo (MC) distribution to a double Gaussian function,

$$g(\Delta t - \Delta t') = a \times e^{-(\Delta t - \Delta t')^2 / 2\sigma_1^2} + b \times e^{-(\Delta t - \Delta t')^2 / 2\sigma_2^2} \quad (90)$$

as shown in Fig. 13. The fitting results were  $\sigma_1 = 0.37\tau_B$ ,  $\sigma_2 = 0.90\tau_B$ , and  $a/b = 4.3$ . The rms of the proper-time difference resolution was 0.68. In the fittings of the proper-time difference, we used two free parameters,  $\text{Im}(\cot \theta)$  and the overall normalization factor.

We used the input values (0.1, 0.3, 0.4) for  $\text{Im}(\cot \theta)$  and tried to visualize how exactly these values are reproduced from the fit. We included the effect of background by assigning the error in the fit as

$$\sigma_i = \sqrt{N_S^i (1 + f_B^i)}$$

for each bin, where  $N_S^i$  and  $f_B^i$  are the number of signals and ratio of the backgrounds to signals for the  $i$ th bin.

## 3. Sensitivity to $\text{Im}(\cot \theta)$

Results of the fit are summarized in Table IV. Result of the fit in the case of  $\text{Im}(\cot \theta) (\text{input}) = 0.1$  is shown in Figs. 14 and 15. It indicates that  $\text{Im}(\cot \theta)$  can be measured with an accuracy of 0.05 corresponding to  $0.87 \text{ fb}^{-1}$  of data. We expect to measure the  $\text{Im}(\cot \theta)$  parameter with a sensitivity of  $\sim 0.005$  with a luminosity of  $100 \text{ fb}^{-1}$ .

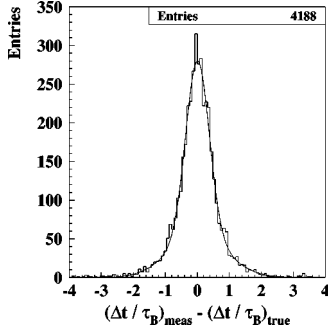


FIG. 13. Resolution for proper time difference.

## G. Determination of $x_d$

### 1. Fitting to proper-time distribution

As described in the previous section, the proper-time distribution for dilepton events contains the information of the mixing parameter  $\Delta m$  (or  $x_d = \Delta m / \Gamma$ ). Figure 16 shows the distributions of the proper-time difference in each category for the same-sign dileptons with the  $P_{c.m.}$  cut at 1.1 GeV/ $c$ . Among the backgrounds, those from continuum [Fig. 16(c)] are assumed to be subtracted using the data taken below  $Y(4S)$ . We fit the proper-time difference distribution with the function

$$F_{\text{tot}}(\Delta\tau) = N_S F_{\text{sig}}(\Delta\tau) + N_B F_{\text{bkg}}(\Delta\tau), \quad (91)$$

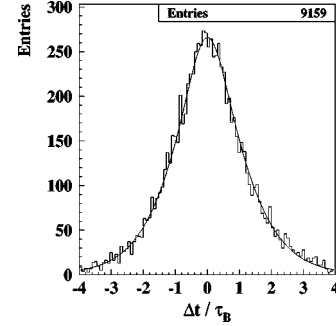
where  $F_{\text{sig}}(\Delta\tau)$  is an observed proper-time difference distribution for signals (SS-1) which is a convolution of the theoretical time evolution and detector resolution functions in the same way as in the opposite-sign dilepton case.  $F_{\text{bkg}}(\Delta\tau)$  is that for backgrounds [SS-2 and SS-3 from  $Y(4S)$ ]. We assumed that this function could be determined by fitting the proper-time difference distribution of the backgrounds with the Monte Carlo simulation. In this analysis, we used the function consisting of double Gaussian and second order polynomial. The fit to the background distribution is also shown in Fig. 16(b).  $N_S$  and  $N_B$  are the normalization for the signals and backgrounds, respectively. The effect of the continuum background was statistically taken into account in the same way as the opposite-sign dilepton case.

### 2. Result

In order to obtain  $x_d$ , we fixed the  $B^0$  lifetime ( $\tau_B$ ) and made a fit with three free parameters ( $x_d$ ,  $N_S$ , and  $N_B$ ). The result of the fit is shown in Fig. 17. With this sample corresponding to the luminosity of  $0.87 \text{ fb}^{-1}$ , we obtained

TABLE IV. Results of the fit to measure  $\text{Im}(\cot \theta)$ .

input $\text{Im}(\cot \theta)$	No. events used in fit	$\text{Im}(\cot \theta)$ from fit
0.1	8732	$0.049 \pm 0.05$
0.3	8830	$0.287 \pm 0.05$
0.4	8855	$0.383 \pm 0.05$


FIG. 14. Simulation result on proper time difference distribution for the signals with  $\text{Im}(\cot \theta) = 0.1$ . The line is the result of fit.

$$x_d = 0.77 \pm 0.061^{+0.020}_{-0.022}, \quad (92)$$

where the first error is a statistical one and the second is a systematic one coming from the error of  $\tau_B = 0.04 \text{ ps}$  (present world average) [18]. We expect the statistical error of  $x_d$  to be 0.006 with a luminosity of  $100 \text{ fb}^{-1}$ . We discuss the systematic error in the next section.

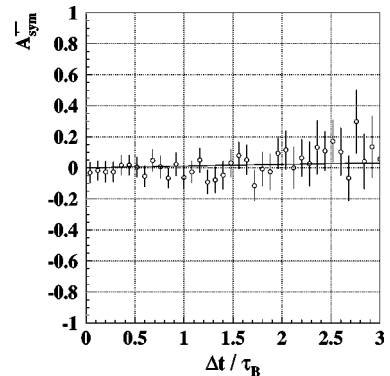
When  $x_d$  is fixed and fit is made for  $\tau_B$ , we obtained with the same sample

$$\tau_B = 1.49 \pm 0.093^{+0.046}_{-0.037} \text{ ps}, \quad (93)$$

where the first error is a statistical one and the second is a systematic one coming from the error of  $x_d = 0.033$  (present world average) [18]. When both  $x_d$  and  $\tau_B$  are taken as free in the fit, errors become much larger because of the large correlation between these two parameters.

## IV. DISCUSSION

We have carried out a simulation study for possible detection of  $CP$  violation and  $CPT$  violation in  $B^0\bar{B}^0$  mixing using the BELLE detector at KEKB. First we derived a general expression for the joint decay rate of the  $B^0\bar{B}^0$  pair produced at  $Y(4S)$  resonance without assuming  $CPT$  invariance. The use of  $(\theta, \phi)$  notation for describing the mixing mass matrix elements, rather than physically straightforward  $M_{ij}$  and  $\Gamma_{ij}$ , simplifies the necessary equations that are used


FIG. 15. Simulation result on  $CPT$  asymmetry. The line shows the asymmetry with  $\text{Im}(\cot \theta) = 0.05$  obtained by the fit to proper-time distribution in Fig. 14.

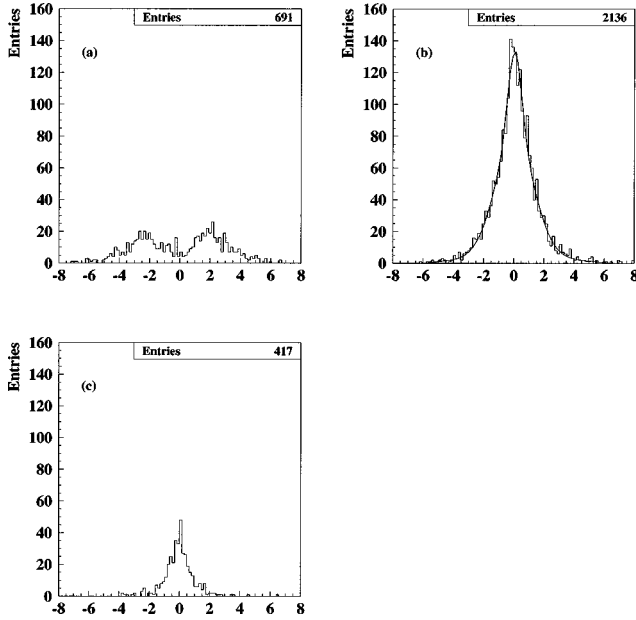


FIG. 16. Distributions of the proper-time difference in each category for the same-sign dileptons with the  $P_{c.m.}$  cut at 1.1 GeV/c. (a) For signal (category SS-1), (b) for background from  $Y(4S)$  (categories SS-2 and SS-3), (c) for background from the continuum events. The curves in (b) are the fit with double Gaussian plus second order polynomial.

here. In this notation,  $CPT$  invariance requires  $\cot \theta = 0$  and  $CP$  invariance requires  $\text{Im}(\phi) = 0$ .

In the same-sign dilepton and single lepton final states  $A_{\text{sym}}^{\ell\ell}$  and  $A_{\text{sym}}^{\ell}$  we use time-integrated charge asymmetries to extract relevant information. Since  $A_{\text{sym}}^{\ell\ell} = \tanh[\text{Im}(\phi)]$  and  $A_{\text{sym}}^{\ell} = \chi_d A_{\text{sym}}^{\ell\ell}$ , we can consider  $A_{\text{sym}}^{\ell}$  as a measurement of  $A_{\text{sym}}^{\ell\ell}$  diluted by the mixing parameter  $\chi_d$ . Their nonzero values are an indication of  $CP$  violation in  $B^0\bar{B}^0$  mixing. The simulation results based on  $100 \text{ fb}^{-1}$  data indicates that we can reach  $\sigma(A_{\text{sym}}^{\ell\ell}) = 0.0066$  and  $\sigma(A_{\text{sym}}^{\ell}) = 0.0006$ . Since the event sample of same-sign dilepton events occupies only a small fraction of the single lepton event sample,  $A_{\text{sym}}^{\ell\ell}$  and  $A_{\text{sym}}^{\ell}$  can be considered as independent. These two mostly

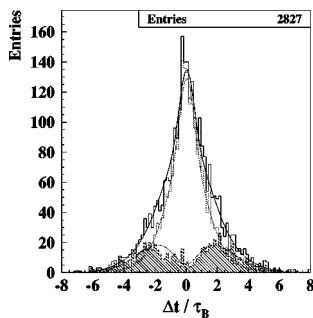


FIG. 17. Distributions of the proper-time difference and fit curve. The solid histogram and line are those for the total (sum of the signal and background) sample. Those for signals (hatched histogram and dot-dash curve) and backgrounds (dotted histogram and curve) are also shown.

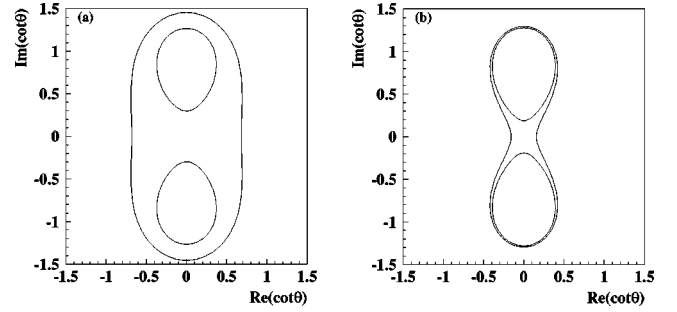


FIG. 18. Allowed region ( $1-\sigma$ ) in the complex  $\cot \theta$  plane obtained from  $\chi$  and  $x_d$  measurements: (a) with the current data (see text), (b) with expected accuracies of 2% for  $\chi$  and 1% for  $x_d$  in the case of  $\text{Im}(\cot \theta) = 0$ . The allowed regions are those containing  $\cot \theta = 0$  for all cases.

independent measurements should in principle help remove some of the possible systematic uncertainties such as those arising from asymmetries in the backgrounds. We combined the two results by converting  $\sigma(A_{\text{sym}}^{\ell\ell}) = 0.0006$  to  $\sigma(A_{\text{sym}}^{\ell}) = 0.004$ , giving an overall sensitivity of  $\sigma(A_{\text{sym}}^{\ell\ell}) = 0.0034$ . While this may not be quite enough for thoroughly covering a region of  $O(10^{-3})$  which is a present prediction of the standard model, some significant fraction of the search region can be covered by the BELLE experiment. Any enhancement to the  $10^{-2}$  level due to new physics can be certainly detected.

In the case of opposite-sign dilepton events, the charge asymmetry has a coefficient  $\text{Im}(\cot \theta)$  in the time-dependent behavior, but the asymmetry vanishes if the time dependence is not measured. Thus a nonzero  $A_{\text{sym}}^{+-}(\Delta t)$  is an indication of  $CPT$  violation in  $B^0\bar{B}^0$  mixing. The BELLE experiment with an accumulation of  $100 \text{ fb}^{-1}$  data will allow a measurement of  $\text{Im}(\cot \theta)$  with a sensitivity of 0.005. The only assumptions we used to reach this conclusion are that  $\cot \theta$  is small enough to neglect  $\cot^2 \theta$  and higher terms, and that  $\Delta\Gamma$  is zero. Both assumptions are considered to be safely valid and there is no known cause to doubt the validity of those assumptions.

Information on  $CPT$ -violation parameter  $\cot \theta$  can also be obtained from the comparison of two parameters which describe the  $B^0\bar{B}^0$  mixing,  $\chi$  and  $x_d$ .  $x_d$  is directly obtained from the time evolution of the same-sign dilepton events, and is independent of  $\cot \theta$ . On the other hand,  $\chi$  depends on  $\cot \theta$  as well as  $x_d$  as seen in Eq. (75). Therefore, comparison of the two independently measured  $\chi$  and  $x_d$  values provides a constraint on  $\cot \theta$ . Figure 18(a) shows the  $1-\sigma$  allowed region in complex  $\cot \theta$  plane obtained from the recent data,  $\chi = 0.149 \pm 0.031$  (CLEO) [10] and  $x_d = 0.722 \pm 0.035$  (CERN  $e^+e^-$  collider LEP average) [18]. Here, we set  $y = 0$  and assume small charge asymmetry of the  $B^0\bar{B}^0$  mixing [ $|e^{\pm i\phi}|^2 \cong 1 \mp 2 \text{Im}(\phi)$ ]. From the simulation study, we expect with  $100 \text{ fb}^{-1}$  data  $\sigma_{x_d}(\text{stat}) \cong 0.006$ . We also expect that the accuracy of  $B^0$  lifetime measurement will improve by a factor of 3 or more and reach to 1% level by then. Presently, the accuracy of  $\chi$  measurement using dilepton events is limited by the uncertainty ( $\sim 15\%$ ) of  $\Lambda$

$\equiv f_+ b_+^2 / (f_+ b_+^2 + f_0 b_0^2)$ , where  $f_+$  ( $f_0$ ) is the fraction of  $B^+ B^-$  ( $B^0 \bar{B}^0$ ) pairs from  $Y(4S)$  and  $b_+$  ( $b_0$ ) is a semileptonic branching ratio of  $B^\pm$  ( $B^0$ ). To avoid the effect of the large uncertainty of  $\Lambda$ , other methods such as partial  $D^* \ell \nu$  reconstruction were also tried by CLEO [10], where a statistical error was the dominant contribution. In both cases, the accuracy of the  $\chi$  measurements are approximately 20% with  $1 \text{ fb}^{-1}$  data. Assuming that the accuracy of the measurements improves inversely with the square-root of the accumulated data, we expect about 2% accuracy in  $\chi$  measurement with  $100 \text{ fb}^{-1}$  data. With the above measurement accuracies, the allowed region in  $\cot \theta$  will be reduced as shown in Fig. 18(b) in the case of  $\text{Im}(\cot \theta) = 0$ . Combining the  $\text{Im}(\cot \theta)$  measurement from  $A_{\text{sym}}^{+-}(\Delta t)$  using the opposite-sign dilepton events, we expect a sensitivity of 0.16 on  $\text{Re}(\cot \theta)$ .

The measurement of the imaginary part of  $\cot \theta$  in the kaon system uses a relation  $\langle K_S | K_L \rangle \sim 2 \text{Re}(\epsilon) - 2i \text{Im}(\delta)$ .  $CPT$  invariance requires  $\delta$  to be zero, and this implies that there is no imaginary part in this amplitude. Here one should be reminded that  $\delta$  is approximately equal to  $(\cot \theta)/2$  for  $\delta \ll 1$  as given in Eq. (17). An assumption that intermediate physical states in the transition between  $K_L$  and  $K_S$  are dominated by the  $I=0$  two-pion state, leads to the expression  $\langle K_S | K_L \rangle \sim 2(\eta_{+-} - \gamma_S^{+-} + \eta_{00} \gamma_S^{00}) / (2i \Delta m_K + \gamma_S + \gamma_L)$ . Here  $\gamma_L$  and  $\gamma_S$  are the total decay widths of  $K_L$  and  $K_S$ ,  $\gamma_S^{+-}$  and  $\gamma_S^{00}$  are the partial decay widths of  $K_S$  into  $\pi^+ \pi^-$  and  $\pi^0 \pi^0$ ,  $\Delta m_K$  is the mass difference between  $K_L$  and  $K_S$ . The currently available data [19] leads to  $\text{Im}(\delta) \sim 2.28 \times 10^{-3} [2/3(\phi_{+-} - \phi_\epsilon) + 1/3(\phi_{00} - \phi_\epsilon)]$ . Here,  $\phi_{+-}$  and  $\phi_{00}$  are the phases of  $\eta^{+-}$  and  $\eta^{00}$ , respectively, and  $\phi_\epsilon$  is the phase of  $\epsilon$ . Both  $\phi_{+-}$  and  $\phi_{00}$  have been measured with an accuracy of an order of one degree. If one uses the superweak phase in place of  $\phi_\epsilon$ , which is defined as  $\phi_{\text{SW}} = \tan^{-1}(2\Delta m_K / \gamma_S)$  and is determined from  $\tau_S$  and  $\Delta m_K$  measurements to an accuracy of a fractional degree, one can attempt to conclude that  $\text{Im}(\delta)$  has been measured to  $10^{-4}$  level in contrast to the  $5 \times 10^{-3}$  level of our proposed analysis. Although the two analyses try to detect the same quantity, namely, the imaginary part of  $\cot \theta$ , a significant difference between the two should be noted. While the method in the  $B^0 \bar{B}^0$  case is straightforward, that of the neutral kaon system assumes  $\phi_\epsilon \sim \phi_{\text{SW}}$ . This is to say that no additional phase other than the superweak phase contributes to  $\phi_\epsilon$ . It has been pointed out that non-negligible contribution to the phase of  $\langle K_S | K_L \rangle$  from the  $I=2$  two-pion state, three-pion state, and semileptonic decays might be present [20].

The real part of  $\cot \theta$  can be measured in the kaon experiment where  $K^0$  and  $\bar{K}^0$  are generated and tagged. Here the time evolution takes an identical expression as described in Sec. II, and the charge asymmetry for semileptonic decays is given by Eq. (69) with  $\Delta t$  replaced by  $t$ . In the case of  $B^0 \bar{B}^0$  the term which contains the real part of  $\cot \theta$  drops out because of the condition  $\Delta \Gamma = 0$ . In the case of neutral kaon system, this condition no longer holds, and  $\text{Re}(\cot \theta)$  can be measured from  $A_{\text{sym}}^{+-}(t)$  in the large  $t$  region, because  $A_{\text{sym}}^{+-}(t)$  becomes  $2 \text{Re}(\cot \theta)$  in the limit  $\Delta \Gamma t \gg 1$ . The first such measurement was done by CPLEAR, giving the result

$\text{Re}(\delta) = [0.07 \pm 0.53(\text{stat}) \pm 0.45(\text{sys})] \times 10^{-3}$  [21]. Similar measurements will be possible in future  $\phi$  factory experiments [22].

The physical consequence of  $CPT$  violation must show up in differences of the mass or the lifetime between a particle and its antiparticle. We can examine the relation between  $\cos \theta$  and those quantities using Eqs. (5) and (12):

$$\begin{aligned} \text{Re}(\cos \theta) &= \frac{\Delta m_0 \Delta m + \frac{1}{4} \Delta \Gamma_0 \Delta \Gamma}{\Delta m^2 + \frac{1}{4} \Delta \Gamma^2} \\ \text{Im}(\cos \theta) &= \frac{1}{2} \frac{\Delta m_0 \Delta \Gamma - \Delta \Gamma_0 \Delta m}{\Delta m^2 + \frac{1}{4} \Delta \Gamma^2}. \end{aligned} \quad (94)$$

Here  $\Delta m_0 \equiv (M_{11} - M_{22})$  and  $\Delta \Gamma_0 \equiv (\Gamma_{11} - \Gamma_{22})$ . We can set  $\cos \theta \approx \cot \theta$  since we assume  $\cos \theta \leq 1$ . In the  $B^0 \bar{B}^0$  system, we can set  $\Delta \Gamma = 0$ . This leads to

$$\text{Re}(\cot \theta) \sim \Delta m_0 / \Delta m, \quad \text{Im}(\cot \theta) \sim -\Delta \Gamma_0 / (2\Delta m). \quad (95)$$

This implies that the  $\text{Im}(\cot \theta)$  measurement gives information about the lifetime difference. The sensitivity of  $5 \times 10^{-3}$  in this analysis translates to a sensitivity of  $\Delta \Gamma_0 / \Gamma \sim \text{several} \times 10^{-3}$  since  $\Delta m$  is of the order of  $\Gamma$ . Information on the mass difference comes from  $\text{Re}(\cot \theta)$  and the sensitivity we can achieve from this analysis is  $\Delta m_0 / \Delta m \sim 0.16$ .

In the case of the kaon system, we use a triangular relation in the complex plane

$$\eta_{+-} = \epsilon - \delta \quad (96)$$

which is derived from the decay amplitudes of  $K_S = K_1 + (\epsilon + \delta)K_2$  and  $K_L = K_2 + (\epsilon - \delta)K_1$  to the  $\pi^+ \pi^-$  state. From this, one can obtain the component of  $\delta$  perpendicular to  $\epsilon$ ,

$$\delta_\perp \approx |\eta_{+-}| (\phi_{+-} - \phi_\epsilon). \quad (97)$$

Solving Eq. (94) for  $\Delta m_0$  and  $\Delta \Gamma_0$ , we obtain

$$\begin{aligned} \Delta m_0 / \Delta m_K &\approx 2 \delta_\perp / \sin \phi_{\text{SW}}, \\ \Delta \Gamma_0 / \gamma_S &\approx -2 \delta_\parallel / \cos \phi_{\text{SW}}, \end{aligned} \quad (98)$$

where we use  $\Delta \Gamma = \gamma_L - \gamma_S \approx -\gamma_S$ . When an assumption  $\phi_\epsilon = \phi_{\text{SW}}$  is made and currently available data are used for  $\delta_\perp$ , one can set a limit  $\Delta m_0 / \Delta m_K \leq 10^{-4}$ . This is better than the sensitivity that is obtained using measurements of  $\text{Re}(\delta)$  and  $\text{Im}(\delta)$ . However, as in the case of the  $\text{Im}(\delta)$  measurement, the validity of assuming  $\phi_\epsilon = \phi_{\text{SW}}$  is a concern. Setting a limit on  $\Delta \Gamma_0$  cannot be done in this analysis and measurements of  $\text{Re}(\delta)$  and  $\text{Im}(\delta)$  are necessary. Currently available data of  $\text{Re}(\delta)$  and  $\text{Im}(\delta)$  set a limit  $\Delta \Gamma_0 / \gamma_S \leq 10^{-3}$ .

As demonstrated in the section of simulation studies, analysis of the lepton events is rather straightforward. The experimental sensitivity that can be reached from the BELLE detector with the  $100 \text{ fb}^{-1}$  data provides valuable information regarding the standard model. For  $CP$  analysis, a large

deviation from the expectation can open a window of new physics. The  $CPT$  analysis of the  $B^0\bar{B}^0$  system has a significant difference compared with the kaon case and the comparison between the two might be interesting.

### ACKNOWLEDGMENTS

We would like to thank M. Kobayashi for useful conversations and for reading the manuscript. One of us (A.M.) would like to thank The Japan Science Society for financial support by the Sasakawa Scientific Research Grant.

### APPENDIX

Here we derive the normalization conditions from the continuity equation of quantum mechanics without assuming  $CPT$  invariance, which are used to eliminate the summation over all final states  $Y$  in the calculation of joint decay rate involving the single lepton final state. We start with the continuity equation

$$\frac{d}{dt}\langle\psi(t)|\psi(t)\rangle = -\sum_Y |\langle Y|\psi(t)\rangle|^2. \quad (\text{A1})$$

Let us take  $\psi(t) = \bar{B}^0$  then from the time evolution of  $\bar{B}^0$  [Eq. (20)]  $\langle\bar{B}^0(t)|\bar{B}^0(t)\rangle$  is obtained as

$$\begin{aligned} \langle\bar{B}^0(t)|\bar{B}^0(t)\rangle &= |f_+(t) - \cos\theta f_-(t)|^2 \\ &+ |\sin\theta e^{-i\phi}|^2 |f_-(t)|^2. \end{aligned} \quad (\text{A2})$$

Using the expressions for  $f_+(t)$  and  $f_-(t)$  from the main text, the above relation can be written in terms of the  $\Delta m$  and  $\Delta\Gamma$  as

$$\begin{aligned} \langle\bar{B}^0(t)|\bar{B}^0(t)\rangle &= \frac{e^{-\Gamma t}}{2} [(1 - |\cos\theta|^2 - |\sin\theta e^{-i\phi}|^2)\cos(\Delta mt) \\ &+ (1 + |\cos\theta|^2 + |\sin\theta e^{-i\phi}|^2)\cosh(\Delta\Gamma t/2) \\ &- i(\cos\theta - \cos\theta^*)\sin(\Delta mt) \\ &- (\cos\theta + \cos\theta^*)\sinh(\Delta\Gamma t/2)]. \end{aligned} \quad (\text{A3})$$

The time derivative of the above equation gives

$$\begin{aligned} \frac{d}{dt}\langle\bar{B}^0(t)|\bar{B}^0(t)\rangle &= -\frac{e^{-\Gamma t}}{2} \left[ \cos(\Delta mt)\{\Gamma(1 - |\cos\theta|^2 - |\sin\theta e^{-i\phi}|^2) + i\Delta m(\cos\theta - \cos\theta^*)\} \right. \\ &+ \cosh(\Delta\Gamma t/2)\left\{\Gamma(1 + |\cos\theta|^2 + |\sin\theta e^{-i\phi}|^2) + \frac{\Delta\Gamma}{2}(\cos\theta + \cos\theta^*)\right\} \\ &- \sin(\Delta mt)\{i\Gamma(\cos\theta - \cos\theta^*) - \Delta m(1 - |\cos\theta|^2 - |\sin\theta e^{-i\phi}|^2)\} \\ &\left. - \sinh(\Delta\Gamma t/2)\left\{\Gamma(\cos\theta + \cos\theta^*) + \frac{\Delta\Gamma}{2}(1 + |\cos\theta|^2 + |\sin\theta e^{-i\phi}|^2)\right\}\right]. \end{aligned} \quad (\text{A4})$$

We now evaluate the right-hand side of Eq. (A1). This is given as

$$\sum_Y |\langle Y|\bar{B}^0(t)\rangle|^2 = \sum_Y |\langle Y|\{[f_+(t) - \cos\theta f_-(t)]\bar{B}^0 + \sin\theta e^{-i\phi} f_-(t)|B^0\}\rangle|^2. \quad (\text{A5})$$

This can be further written as

$$\begin{aligned} \sum_Y |\langle Y|\bar{B}^0(t)\rangle|^2 &= \sum_Y [|f_+(t)|^2 |\bar{A}_Y|^2 + |f_-(t)|^2 \{|\cos\theta|^2 |\bar{A}_Y|^2 + |\sin\theta e^{-i\phi}|^2 |A_Y|^2 \\ &- \sin\theta^* e^{i\phi^*} \cos\theta \bar{A}_Y A_Y^* - \sin\theta e^{-i\phi} \cos\theta^* A_Y \bar{A}_Y^*\} \\ &+ f_+(t) f_-(t)^* \{-\cos\theta^* |\bar{A}_Y|^2 + \sin\theta^* e^{i\phi^*} \bar{A}_Y A_Y^*\} \\ &+ f_-(t) f_+(t)^* \{-\cos\theta |\bar{A}_Y|^2 + \sin\theta e^{-i\phi} \bar{A}_Y^* A_Y\}]. \end{aligned} \quad (\text{A6})$$

Substituting the values of  $f_+(t)$  and  $f_-(t)$  the above expression can be written in terms of  $\Delta m$  and  $\Delta\Gamma$  as

$$\begin{aligned}
\sum_Y |\langle Y|\bar{B}^0(t)\rangle|^2 = & \frac{e^{-\Gamma t}}{2} \sum_Y [\cos(\Delta mt)\{(1-|\cos \theta|^2)|\bar{A}_Y|^2 - |\sin \theta e^{-i\phi}|^2|A_Y|^2 + \sin \theta^* e^{i\phi^*} \cos \theta \bar{A}_Y A_Y^* \\
& + \sin \theta e^{-i\phi} \cos \theta^* A_Y \bar{A}_Y^*\} + \cosh(\Delta\Gamma t/2)\{(1+|\cos \theta|^2)|\bar{A}_Y|^2 + |\sin \theta e^{-i\phi}|^2|A_Y|^2 \\
& - \sin \theta^* e^{i\phi^*} \cos \theta \bar{A}_Y A_Y^* - \sin \theta e^{-i\phi} \cos \theta^* A_Y \bar{A}_Y^*\} + i \sin(\Delta mt)\{(-\cos \theta + \cos \theta^*)|\bar{A}_Y|^2 \\
& + \sin \theta e^{-i\phi} A_Y \bar{A}_Y^* - \sin \theta^* e^{i\phi^*} \bar{A}_Y A_Y^*\} + \sinh(\Delta\Gamma t/2)\{-(\cos \theta + \cos \theta^*)|\bar{A}_Y|^2 + \sin \theta^* e^{i\phi^*} \bar{A}_Y A_Y^* \\
& + \sin \theta e^{-i\phi} A_Y \bar{A}_Y^*\}]. \tag{A7}
\end{aligned}$$

Equating the coefficients of  $\cos(\Delta mt)$ ,  $\cosh(\Delta\Gamma t/2)$ ,  $\sin(\Delta mt)$ , and  $\sinh(\Delta\Gamma t/2)$  one gets the following conditions:

$$\begin{aligned}
\sum_Y \{(1-|\cos \theta|^2)|\bar{A}_Y|^2 - |\sin \theta e^{-i\phi}|^2|A_Y|^2 + \sin \theta^* e^{i\phi^*} \cos \theta \bar{A}_Y A_Y^* + \sin \theta e^{-i\phi} \cos \theta^* A_Y \bar{A}_Y^*\} \\
= \Gamma(1-|\cos \theta|^2 - |\sin \theta e^{-i\phi}|^2) + i\Delta m(\cos \theta - \cos \theta^*), \tag{A8}
\end{aligned}$$

$$\begin{aligned}
\sum_Y \{(1+|\cos \theta|^2)|\bar{A}_Y|^2 + |\sin \theta e^{-i\phi}|^2|A_Y|^2 - \sin \theta^* e^{i\phi^*} \cos \theta \bar{A}_Y A_Y^* - \sin \theta e^{-i\phi} \cos \theta^* A_Y \bar{A}_Y^*\} \\
= \Gamma(1+|\cos \theta|^2 + |\sin \theta e^{-i\phi}|^2) + \frac{\Delta\Gamma}{2}(\cos \theta + \cos \theta^*), \tag{A9}
\end{aligned}$$

$$\begin{aligned}
\sum_Y \{(-\cos \theta + \cos \theta^*)|\bar{A}_Y|^2 + \sin \theta e^{-i\phi} A_Y \bar{A}_Y^* - \sin \theta^* e^{i\phi^*} \bar{A}_Y A_Y^*\} \\
= -\Gamma(\cos \theta - \cos \theta^*) - i\Delta m(1-|\cos \theta|^2 - |\sin \theta e^{-i\phi}|^2), \tag{A10}
\end{aligned}$$

$$\sum_Y \{(\cos \theta + \cos \theta^*)|\bar{A}_Y|^2 - \sin \theta^* e^{i\phi^*} \bar{A}_Y A_Y^* - \sin \theta e^{-i\phi} A_Y \bar{A}_Y^*\} = \Gamma(\cos \theta + \cos \theta^*) + \frac{\Delta\Gamma}{2}(1+|\cos \theta|^2 + |\sin \theta e^{-i\phi}|^2). \tag{A11}$$

Taking  $\psi(t) = B^0(t)$  in the continuity equation given in Eq. (A1) and exactly following the same procedure, a set of relations corresponding to those obtained in Eqs. (A8)–(A11) are found to be

$$\begin{aligned}
\sum_Y \{(1-|\cos \theta|^2)|A_Y|^2 - |\sin \theta e^{i\phi}|^2|\bar{A}_Y|^2 - \sin \theta^* e^{-i\phi^*} \cos \theta A_Y \bar{A}_Y^* - \sin \theta e^{i\phi} \cos \theta^* \bar{A}_Y A_Y^*\} \\
= \Gamma(1-|\cos \theta|^2 - |\sin \theta e^{i\phi}|^2) - i\Delta m(\cos \theta - \cos \theta^*), \tag{A12}
\end{aligned}$$

$$\begin{aligned}
\sum_Y \{(1+|\cos \theta|^2)|A_Y|^2 + |\sin \theta e^{i\phi}|^2|\bar{A}_Y|^2 + \sin \theta^* e^{-i\phi^*} \cos \theta A_Y \bar{A}_Y^* + \sin \theta e^{i\phi} \cos \theta^* \bar{A}_Y A_Y^*\} \\
= \Gamma(1+|\cos \theta|^2 + |\sin \theta e^{i\phi}|^2) - \frac{\Delta\Gamma}{2}(\cos \theta + \cos \theta^*), \tag{A13}
\end{aligned}$$

$$\sum_Y \{(\cos \theta - \cos \theta^*)|A_Y|^2 + \sin \theta e^{i\phi} \bar{A}_Y A_Y^* - \sin \theta^* e^{-i\phi^*} A_Y \bar{A}_Y^*\} = \Gamma(\cos \theta - \cos \theta^*) - i\Delta m(1-|\cos \theta|^2 - |\sin \theta e^{i\phi}|^2), \tag{A14}$$

$$\sum_Y \{(\cos \theta + \cos \theta^*)|A_Y|^2 + \sin \theta^* e^{-i\phi^*} A_Y \bar{A}_Y^* + \sin \theta e^{i\phi} \bar{A}_Y A_Y^*\} = \Gamma(\cos \theta + \cos \theta^*) - \frac{\Delta\Gamma}{2}(1+|\cos \theta|^2 + |\sin \theta e^{i\phi}|^2). \tag{A15}$$

From the above relations, the normalizations of decay amplitudes are given as

$$\sum_Y |A_Y|^2 = \Gamma + \Delta m \operatorname{Im}(\cos \theta) - \frac{\Delta\Gamma}{2} \operatorname{Re}(\cos \theta) \quad (\text{A16})$$

$$\sum_Y |\bar{A}_Y|^2 = \Gamma - \Delta m \operatorname{Im}(\cos \theta) + \frac{\Delta\Gamma}{2} \operatorname{Re}(\cos \theta), \quad (\text{A17})$$

$$\begin{aligned} & \sum_Y \{ \sin \theta^* e^{i\phi^*} A_Y^* \bar{A}_Y - \sin \theta e^{-i\phi} A_Y \bar{A}_Y^* \} \\ &= i\Delta m (1 - |\cos \theta|^2 - |\sin \theta e^{-i\phi}|^2) + 2i \operatorname{Im}(\cos \theta) \\ & \times \left[ \Delta m \operatorname{Im}(\cos \theta) - \frac{\Delta\Gamma}{2} \operatorname{Re}(\cos \theta) \right], \quad (\text{A18}) \end{aligned}$$

$$\begin{aligned} & \sum_Y \{ \sin \theta^* e^{i\phi^*} A_Y^* \bar{A}_Y + \sin \theta e^{-i\phi} A_Y \bar{A}_Y^* \} \\ &= -\frac{\Delta\Gamma}{2} (1 + |\cos \theta|^2 + |\sin \theta e^{-i\phi}|^2) \\ & - 2 \operatorname{Re}(\cos \theta) \left[ \Delta m \operatorname{Im}(\cos \theta) - \frac{\Delta\Gamma}{2} \operatorname{Re}(\cos \theta) \right]. \quad (\text{A19}) \end{aligned}$$

If  $CPT$  is conserved, the above expressions reduce to

$$\sum_Y |A_Y|^2 = \Gamma, \quad (\text{A20})$$

$$\sum_Y |\bar{A}_Y|^2 = \Gamma, \quad (\text{A21})$$

$$\sum_Y \{ e^{i\phi^*} A_Y^* \bar{A}_Y - e^{-i\phi} A_Y \bar{A}_Y^* \} = i\Delta m (1 - |e^{-i\phi}|^2), \quad (\text{A22})$$

$$\sum_Y \{ e^{i\phi^*} A_Y^* \bar{A}_Y + e^{-i\phi} A_Y \bar{A}_Y^* \} = -\frac{\Delta\Gamma}{2} (1 + |e^{-i\phi}|^2). \quad (\text{A23})$$

- 
- [1] J. H. Christenson, J. W. Cronin, V. L. Fitch, and R. Turlay, *Phys. Rev. Lett.* **13**, 138 (1964).  
[2] M. Kobayashi and T. Maskawa, *Prog. Theor. Phys.* **49**, 652 (1973).  
[3] J. Hagelin, *Phys. Rev. D* **20**, 2893 (1979); *Nucl. Phys.* **B193**, 123 (1981).  
[4] M. Lusignoli, *Z. Phys. C* **41**, 645 (1989); A. Acuto and D. Cocolicchio, *Phys. Rev. D* **47**, 3945 (1993).  
[5] J. Ellis *et al.*, *Nucl. Phys.* **B304**, 205 (1988).  
[6] T. Altomari, L. Wolfenstein, and J. Bjorken, *Phys. Rev. D* **37**, 1860 (1988).  
[7] I. I. Bigi and A. I. Sanda, *Nucl. Phys.* **B281**, 41 (1987); D. Cocolicchio and L. Maiani, *Phys. Lett. B* **291**, 155 (1992); A. I. Sanda and Z. Z. Xing, *Phys. Rev. D* **56**, 6866 (1997).  
[8] A. J. Buras, W. Slominski, and H. Steger, *Nucl. Phys.* **B245**, 369 (1984).  
[9] H. Yamamoto, *Phys. Lett. B* **401**, 91 (1997).  
[10] J. Bartelt *et al.*, *Phys. Rev. Lett.* **71**, 1680 (1993).  
[11] M. Kobayashi and A. I. Sanda, *Phys. Rev. Lett.* **69**, 3139 (1992).  
[12] R. Carosi *et al.*, *Phys. Lett. B* **237**, 303 (1990).  
[13] Z. Z. Xing, *Phys. Rev. D* **50**, 2957 (1994); D. Collady and V. A. Kostelecky, *Phys. Lett. B* **344**, 259 (1995); V. A. Kostelecky and R. V. Kooten, *Phys. Rev. D* **54**, 5585 (1996).  
[14] KEKB B-Factor design report, KEK Report No. 95-7, 1995.  
[15] BELLE technical design report, KEK Report No. 95-1, 1995.  
[16] BaBar technical design report, Report No. SLAC-R-95-457, 1995.  
[17] T. D. Lee and C. S. Wu, *Annu. Rev. Nucl. Sci.* **16**, 471 (1966).  
[18] R. Forty, talk presented at *B Physics and CP Violation Conference*, 1997, Honolulu, Hawaii (unpublished).  
[19] Particle Data Group, R. M. Barnett *et al.*, *Phys. Rev. D* **54**, 1 (1996).  
[20] L. Lavoura, *Ann. Phys. (N.Y.)* **207**, 428 (1991).  
[21] L. Tauscher *et al.*, *Nucl. Phys. B (Proc. Suppl.)* **59**, 182 (1997).  
[22] M. Fukawa *et al.*, KEK Report No. 90-12, 1990 (unpublished); C. D. Buchanan *et al.*, *Phys. Rev. D* **45**, 4088 (1992); G. D'Ambrosio *et al.*, in *The Second DAΦNE Physics Handbook*, edited by L. Maiani *et al.* (LNF, Frascati, 1995), p. 63.